NASA TECHNICAL NOTE

NASA TN D-6469

HIGH-ALTITUDE FLIGHT TEST OF A REEFED 12.2-METER-DIAMETER DISK-GAP-BAND PARACHUTE WITH DEPLOYMENT AT A MACH NUMBER OF 2.58

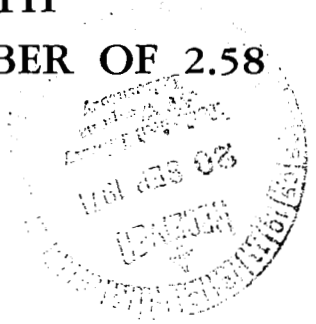

by John S. Preisser and R. Bruce Grow

Langley Research Center
Hampton, Va. 23365

NATIONAL AERONAUTICS AND SPACE ADMINISTRATION • WASHINGTON, D. C. • SEPTEMBER 1971

1. Report No.	2. Government Accession No.	3. Recipient's Catalog No.
NASA TN D-6469		

4. Title and Subtitle	5. Report Date
HIGH-ALTITUDE FLIGHT TEST OF A REEFED 12.2-METER-DIAMETER DISK-GAP-BAND PARACHUTE WITH DEPLOYMENT AT A MACH NUMBER OF 2.58	September 1971
	6. Performing Organization Code
7. Author(s)	8. Performing Organization Report No.
John S. Preisser and R. Bruce Grow	L-7772
	10. Work Unit No.
9. Performing Organization Name and Address	117-07-04-01
NASA Langley Research Center Hampton, Va. 23365	11. Contract or Grant No.
	13. Type of Report and Period Covered
12. Sponsoring Agency Name and Address	Technical Note
National Aeronautics and Space Administration Washington, D.C. 20546	14. Sponsoring Agency Code

15. Supplementary Notes

Technical Film Supplement L-1106 available on request.

16. Abstract

A reefed 12.2-meter nominal-diameter (40-ft) disk-gap-band parachute was flight tested as part of the NASA Supersonic High Altitude Parachute Experiment (SHAPE) program. A three-stage rocket was used to drive an instrumented test payload to an altitude of 43.6 km (143 000 ft) and a Mach number of 2.58 where the parachute was deployed by means of a mortar. After a time delay of about 8.5 seconds, the parachute was disreefed at a Mach number of 0.99. The report contains an analysis of parachute inflation, drag, and stability for both the reefed and unreefed parts of the test. In addition, detailed descriptions of the test parachute, the reefing system, and the parachute packing procedure are included.

17. Key Words (Suggested by Author(s))	18. Distribution Statement
Disk-gap-band parachutes High-altitude parachute tests Reefed parachute tests	Unclassified – Unlimited

19. Security Classif. (of this report)	20. Security Classif. (of this page)	21. No. of Pages	22. Price*
Unclassified	Unclassified	64	$3.00

*For sale by the National Technical Information Service, Springfield, Virginia 22151

HIGH-ALTITUDE FLIGHT TEST OF A REEFED 12.2-METER-DIAMETER DISK-GAP-BAND PARACHUTE WITH DEPLOYMENT AT A MACH NUMBER OF 2.58

By John S. Preisser and R. Bruce Grow
Langley Research Center

SUMMARY

A reefed 12.2-meter nominal-diameter (40-ft) disk-gap-band parachute was flight tested as part of the NASA Supersonic High Altitude Parachute Experiment (SHAPE) program. A three-stage rocket was used to drive the instrumented payload to an altitude of 43.6 km (143 000 ft), a Mach number of 2.58, and a dynamic pressure of 972 N/m^2 (20.3 lb/ft^2) where the parachute was deployed by means of a mortar. The parachute deployed satisfactorily and reached a partially inflated condition characterized by irregular variations in parachute projected area. A full, stable reefed inflation was achieved when the system had decelerated to a Mach number of about 1.5. The steady, reefed projected area was 49 percent of the steady, unreefed area and the average drag coefficient was 0.30. Disreefing occurred at a Mach number of 0.99 and a dynamic pressure of 81 N/m^2 (1.7 lb/ft^2). The parachute maintained a steady inflated shape for the remainder of the deceleration portion of the flight and throughout descent. During descent, the average effective drag coefficient was 0.57. There was little, if any, coning motion, and the amplitude of planar oscillations was generally less than 10^o.

INTRODUCTION

The NASA Supersonic High Altitude Parachute Experiment (SHAPE) program is a continuation of the earlier NASA Planetary Entry Parachute Program (PEPP) (refs. 1 and 2) designed to study parachute performance in low-density environments. The test conditions of interest for PEPP and SHAPE were supersonic Mach numbers and relatively low dynamic pressures such as might be encountered during a Mars landing mission.

This report presents flight data and an analysis of a 12.2-meter nominal-diameter (40-ft) disk-gap-band (DGB) parachute which was deployed at a Mach number of 2.58 and a dynamic pressure of 972 N/m^2 (20.3 lb/ft^2). The parachute was deployed in a reefed condition by means of a mortar and was disreefed several seconds later. The main purpose of the test was to study the effect of reefing on parachute performance. A reefing-line length was chosen which gave the same reefing geometry as a wind-tunnel model

(ref. 3) which exhibited about 50 percent less drag than an unreefed model and which had good stability at supersonic Mach numbers. A reefed parachute having 50 percent of the unreefed drag has been considered for one stage of a multistage decelerator system for a Mars entry mission, primarily as a means of reducing the maximum opening load. Also, it was desired to investigate whether reefing would diminish large canopy area fluctuations that had previously been encountered during flight tests at high Mach numbers. The parachute for the test reported herein was constructed with Nomex cloth in the center section of the canopy disk, since aerodynamic heating had damaged that area of a DGB which was fabricated of dacron material and deployed at a Mach number of 3.31. (See ref. 4.)

A reefed DGB was flight tested earlier in the SHAPE program, but the reefing attachment system failed. A brief discussion of the results of that test is presented in appendix A of this report. The attachment system was subsequently modified for the test described in this report.

A detailed description of the procedure used to pack the parachute prior to flight is presented in appendix B. This procedure is the result of cumulative experience gained during the PEPP and SHAPE programs.

Motion-picture film supplement L-1106 is available on loan; a request card and description of the film are included at the back of this paper.

SYMBOLS

Throughout this report, the International System of Units is used, followed by the British Engineering System of Units in parentheses. However, the British system was used for all measurements and calculations.

a_x linear acceleration along longitudinal axis of payload, g-units

$C_{A,o}$ nominal axial-force coefficient

$C_{D,o}$ drag coefficient, average of calculated $C_{A,o}$ values

$(C_{D,o})_{eff}$ effective drag coefficient (based on vertical descent velocity and acceleration)

D_o nominal diameter, $\left(\frac{4S_o}{\pi}\right)^{1/2}$, meters (ft)

g acceleration due to gravity, 9.81 m/sec^2 (32.2 ft/sec^2)

M	Mach number
m	total mass of payload and parachute, kg (slugs)
Δp	differential pressure, cm H_2O (in. H_2O)
q_∞	free-stream dynamic pressure, $\frac{1}{2}\rho_\infty V^2$, N/m^2 (lb/ft^2)
S_o	nominal surface area of parachute canopy including gap and vent, $meters^2$ (ft^2)
S_p	projected area of parachute canopy, $meters^2$ (ft^2)
$S_{p,final}$	projected area of parachute canopy at steady, unreefed, full inflation, $meters^2$ (ft^2)
t	time from vehicle lift-off, sec
t'	time from mortar firing, sec
V	true airspeed, m/sec (ft/sec)
X, Y, Z	payload body-axis system
X_f, Y_f, Z_f	earth-fixed axis system
Z_E	local vertical axis, positive down $(Z_E = X_f)$
δ_E	payload resultant pitch-yaw angle from local vertical, deg
θ, ψ, φ	gyro platform angles relating body-axis system to inertial coordinate system (gyro-uncaging position), deg
$\theta_E, \psi_E, \varphi_E$	Euler angles relating body-axis system to earth-fixed axis system, deg
ρ	atmospheric density, kg/m^3 ($slugs/ft^3$)

Subscripts:

meas	measured
std	standard
∞	free stream

Dots over symbols denote differentiation with respect to time.

TEST SYSTEM

Launch Vehicle System

An Honest John-Nike-Nike rocket combination was used to propel the payload to the proper altitude and velocity for the desired test. When the test conditions were reached, a radio command was sent to start onboard cameras and a programer. After a time delay of about 1 second, the programer initiated the firing of a mortar which deployed the parachute. A photograph of the rocket vehicle in the launch position is presented as figure 1. A photograph of the test payload attached to the rocket vehicle is shown as figure 2. The payload was 155 cm (61 in.) long and the diameter of the cylindrical portion was 34.3 cm (13.5 in.). The payload was built with three equally spaced external pods (two of which are visible in fig. 2). (Their purpose is discussed later.) The parachute, instrumentation, and a telemetry system were all contained within the payload.

Deployment System

The parachute was packed in a split cylindrical bag and then placed in the mortar tube which was located at the aft end of the payload. (For details concerning the parachute packing procedure, refer to appendix B.) The mouth of the bag was inserted in the mortar first and rested on the mortar sabot (deployment piston). The packed parachute fits completely into the mortar tube. The mortar lid, or cover, which was fastened to the bottom of the deployment bag, was held to the mortar tube by means of shear pins and thus held the packed parachute in place. A lines-first-type deployment method was used. That is, after ejection from the mortar the suspension lines would deploy from the bag first and would be followed by the canopy. The bag-cover combination was permanently attached to the canopy apex to eliminate the danger of damage to the parachute from the free-flying bag-cover combination as had previously occurred (ref. 5).

Instrumentation

The onboard instrumentation included a tensiometer, four accelerometers, an attitude reference system, and two cameras. The tensiometer used a strain-gage bridge as the sensing element and was placed in the parachute attachment system to measure the force between the payload and the parachute. The tensiometer was ranged from 0 to 44.5 kN (0 to 10 000 lb). Payload accelerations were measured by servo accelerometers having capacitance sensors. Two accelerometers were alined with the longitudinal axis of the payload; one was scaled to ±75 g-units, the other to ±5 g-units. The remaining two accelerometers were mounted normal to the payload longitudinal axis and normal to each other. These normal accelerometers were scaled to ±5 g-units. The attitude reference system, hereafter referred to as a gyro platform, measured the pitch, yaw, and roll attitude of the payload in flight relative to an inertial reference (the gyro uncage position on the launcher). One of the two payload cameras was mounted in a payload pod and pointed aft so that it would view the parachute. The other camera was mounted in the nose of the payload and pointed forward through a quartz window. (See fig. 2.)

The tensiometer, accelerometer, and gyro platform data were telemetered to ground receiving stations. The film was recovered with the payload after the flight. Coded timing appeared on both the camera film and telemetry data and was used to correlate the two.

Backup Recovery System

The payload also contained two 3.05-meter (10-ft) ribbon parachutes which were placed in the remaining two of the three external pods on the payload. (See fig. 2.) These parachutes could have been deployed by radio command if the test parachute failed to deploy or inflate, or if it were damaged to such an extent that the impact velocity would likely cause damage to the payload.

TEST PARACHUTE

Geometric Description

The test parachute was a disk-gap-band design. The "disk" is a regular polygon with 32 sides (nearly a circle). The "band" is a right circular cylinder circumscribing the disk. The "gap" is an open area between the band and the disk. There was an open area or vent in the center of the disk as well. A reefing system was attached to the inside surface of the canopy at the disk-gap junction.

The nomenclature used throughout this report in describing the parachute and the system used to attach the parachute to the test payload is presented in figure 3 along with

a schematic view of two opposing gores of the canopy. The parachute was constructed from 16 pairs of opposing gores. The gores were sewn together with bias seams to form the parachute canopy. The principal dimensions of one of the 32 gores are shown in figure 4. Geometric characteristics of the test parachute system are presented in table I.

The parachute had a nominal diameter of 12.2 meters (40 ft) based on a nominal area of 116.7 meters^2 (1256 ft^2). The nominal area (S_o) is equal to the sum of the surface areas of the disk (S_D), gap (S_G), and band (S_B); that is,

$$S_o = S_D + S_G + S_B$$

The surface area of the disk (which includes the vent) is given by

$$S_D = nl \frac{r}{2} \cos\left(\frac{180^o}{n}\right)$$

where

n number of sides (or gores)

l length of each side

r radius of circumscribed circle

The surface area of the band is

$$S_B = nlH_B$$

where H_B is the height of the band. The surface area of the gap is

$$S_G = nlH_G$$

where H_G is the height of the gap. The gap and vent provided a total open area or geometric porosity of 12.5 percent of S_o. There were 32 suspension lines, each of which attached to a radial tape at the bottom edge of the band. The suspension lines were 12.2 meters (40 ft) or $1.0D_o$ long.

Reefing System

The test parachute was equipped with a reefing system, part of which is shown in figure 5. The reefing system included 29 reefing rings, 3 reefing-line cutters secured in

brackets, and the reefing line. As shown in figure 5, the reefing line was attached to each radial tape at the disk hem by the reefing rings or the reefing-line cutter brackets.

The reefing rings had an outside diameter of 1.8 cm, an inside diameter of 1.4 cm, and a width of 0.76 cm (0.70 in., 0.55 in., and 0.30 in., respectively). The rings were made of stainless steel. They were attached to the inside surface of the canopy at the intersection of the disk hem and the radial tape by sewing through all the material at that junction. This method of attachment differs from that of the previous reefed test. (See appendix A.)

The reefing-line cutters were pyrotechnic devices which included an 8-second delay train. The delay train was initiated by the pulling of a lanyard which occurred at the time of the first relative motion between the top of the parachute band and the parachute disk. This condition occurred immediately after suspension line stretch during the parachute deployment when the canopy skirt started to emerge from the bag (see appendix B). The three reefing cutters were mounted in brackets which were nearly equally spaced around the circumference of the disk. The brackets were attached to the canopy in a manner similar to the ring attachment.

The reefing line was a single piece of braided dacron cord with a rated tensile strength of 8900 N (2000 lb). After the reefing line was threaded through the rings and cutters, the ends were spliced together to form a 3.42-m-diameter (11.2-ft) reefing-line loop.

Figure 6 is a sketch of the flight configuration for both the reefed and unreefed parachute. The parachute dimensions that are indicated were obtained from the aft camera film. First, enlargements were made of individual frames and then a polymeter was used to obtain the projected areas of the reefing-line loop, the disk, and the entire parachute. Diameters were calculated by assuming the areas to be circular and from a knowledge of the actual diameter of the reefing-line loop. All diameters were then graphically projected into their respective planes to obtain the dimensions shown in figure 6. They are believed to be accurate to within 0.2 meter (0.6 ft).

Material and Weights

One of the principal considerations in selecting materials for the fabrication of the test parachute was the requirement that all materials used be capable of maintaining structural integrity and geometric size when subjected to a temperature of 135^{o} C for more than 100 hours (sterilization requirement for interplanetary flight). Therefore, most of the cloth material used was dacron instead of nylon, as is commonly used. In addition, a low-shrinkage, heat-stabilized dacron thread was used for sewing the parachute together. Nomex cloth was used in the center or crown portion of the disk on this parachute (see fig. 4) because of the degradation of structural strength experienced in

dacron cloth in the crown of a similar parachute in a previous test (ref. 4). That strength deterioration was attributed to aerodynamic heating.

Table II lists the characteristics of the materials used in the fabrication of the test parachute. Materials were selected from those which were commercially available at the time of fabrication. For this reason, some of the materials used were stronger and heavier than that dictated by design requirements. The values shown in the table were measured, except as noted otherwise. The weight breakdown of the parachute system is presented in table III.

RESULTS AND DISCUSSION

Test Data

Vehicle lift-off occurred at 11:15 a.m. MDT, on June 20, 1970 at White Sands Missile Range, New Mexico. The flight sequence and recorded times for significant events are presented in figure 7. Altitude and velocity time histories for the first 360 seconds of flight are shown in figure 8. As shown by the figures, the payload was ascending at the time of parachute deployment. The primary test period is contained within the first 20 seconds after parachute deployment and hereafter will be referred to as the deceleration part of the test. The postapogee period will be referred to as the descent part of the test.

A radiosonde was released near the time of the test and a sounding rocket was launched about 1 hour later to provide atmospheric density and wind profiles. The resulting density data, expressed as a ratio to the 1962 U.S. Standard Atmosphere (ref. 6) are presented in figure 9 and the wind data are presented in figure 10.

The measured atmospheric properties were used with velocity data determined from FPS-16 radar tracking information and telemetered accelerometer data to determine the payload true airspeed, Mach number, and dynamic pressure (figs. 11 and 12) during the deceleration part of the test. Parachute deployment was initiated by mortar firing and is designated by $t' = 0$ in the figures. At the time of mortar firing, the payload was at an altitude of 43.6 km (143 000 ft) and, as indicated in figures 11 and 12, the Mach number was 2.58 and the dynamic pressure was 972 N/m^2 (20.3 lb/ft^2). The estimated uncertainties in the deployment conditions are ±0.046 km (±150 ft) in altitude, ±0.04 in Mach number, and ±34 N/m^2 (±0.7 lb/ft^2) in dynamic pressure, based on a first-order error analysis using a ±7.6 m/s (±25 ft/s) velocity error, a 2-percent temperature error, and a 3-percent density error. Parachute disreef occurred at $t' = 8.49$ seconds. At the time of disreef, the payload-parachute system was at an altitude of 48.1 km (157 650 ft), a Mach number of 0.99, and a dynamic pressure of 81 N/m^2 (1.7 lb/ft^2). Estimated uncertainties

in the disreef conditions are ±0.046 km (±150 ft), ±0.03, and ±5 N/m^2 (±0.1 lb/ft^2) for the altitude, Mach number, and dynamic pressure, respectively.

The relative force between the parachute and payload as measured by the tensiometer during the deceleration part of the test is presented in figure 13. Note that an insert showing an expanded time scale also appears in the figure. The first peak load of 4492 N (1010 lb) at 0.17 second (noted by ① in fig. 13) occurred when the parachute attachment system first became fully extended. At this time, the parachute riser and a small part of the suspension lines were out of the deployment bag which was traveling rearward relative to the payload. The second peak load of 9697 N (2180 lb) at 0.44 second (noted by ②) occurred when the suspension lines were deployed and the parachute skirt began to emerge from the bag. This load is commonly referred to as the snatch force. The next peak load of 16 991 N (3820 lb) at 0.76 second (noted by ③) occurred when the disk part of the canopy first became fully inflated. The maximum load of 22 107 N (4970 lb) occurred two cycles later at 0.96 second (noted by ④). The high-frequency (approximately 10 Hz) character of the tensiometer history for the first several seconds resulted from a longitudinal oscillation in the elastic suspension lines. This oscillatory behavior had also been observed in earlier flight tests such as those of references 4 and 5. Disreefing occurred at 8.49 seconds (noted by ⑤) and was characterized by a momentary drop in the load that was followed by a sharp rise to an 8807 N (1980 lb) peak 0.08 second later. Thereafter, the load decayed fairly smoothly. The uncertainty in the tensiometer data is about ±445 N (±100 lb).

Figure 14 presents the data from the ±75 g-unit longitudinal accelerometer, the ±5 g-unit longitudinal accelerometer, and the two ±5 g-unit accelerometers mounted normal to them. Normal accelerations were small and the longitudinal accelerations closely agree with the tensiometer history of figure 13. The ±5 g-unit accelerometer was off scale for most of the first 6 seconds and thereafter agrees with the ±75 g-unit results but with less noise and greater accuracy. All accelerometers are considered to be accurate to within 1 percent of their full-scale value.

The payload attitude in flight was measured by the gyro platform. These angles were measured in an Euler angle sequence of pitch, yaw, and roll and were referenced to the attitude of the payload at the time of gyro uncaging. The gyro was uncaged prior to vehicle lift-off at the launch elevation but at an azimuth which was offset from the launch azimuth. The offset azimuth was intended to counter the effects of high-altitude winds near flight apogee which could cause the gyro to exceed its yaw operating limit (±85°) and tumble. The gyro offset procedure is discussed in detail in reference 7. Time histories of pitch and yaw for the payload during the deceleration period after mortar firing are shown in figure 15. Prior to mortar firing, pitch and yaw rates were near zero. Mortar firing induced a slight pitch and yaw rate (less than 10° per second). After initial

parachute inflation and during the time of unsteady loading when suspension-line longitudinal oscillations were severe, pitch and yaw rates were large and became as high as 250° per second. (See yaw at 1.5 seconds.) After disreef when the loading was steady, the angular rates were again small. After investigation of the aft camera film, it was determined that during the reefed, unsteady loading portion of the test, the payload pitch and yaw motion was primarily about the parachute axis of symmetry near the point where the three legs of the bridle were joined. During the unreefed, steady portion of the deceleration, a longer period motion was present along with a superimposed short-period oscillation. The longer period motion was associated with the payload and parachute acting together like a rigid system, whereas the short-period motion was about the parachute axis.

The roll angle of the payload as measured by the gyro platform and the roll angle of the parachute relative to earth-fixed axes as determined from the aft camera film are presented in figure 16. The payload had a slight roll rate of about 0.15 revolution per second at the time of mortar firing. Shortly after reefed inflation, the roll motion reversed direction but remained at a small rate (0.1 revolution per second or less). The parachute canopy had even less roll but it was in a direction opposite to that of the payload. The swivel in the riser system allowed different roll rates for the payload and the parachute, but provided little damping.

Analysis of Parachute Performance

Deployment.- The test parachute was mortar deployed. There was little or no payload tipoff. The reaction load on the payload was an average of 25 g-units for approximately 0.03 second with a peak of 39 g-units. The bridle and riser systems were fully extended in 0.17 second. Suspension line stretch occurred at 0.44 second. The time at which the parachute canopy reached full-length deployment could not be determined from the aft camera film. However, the canopy vent is first visible on the film at 0.62 second; therefore, full-length deployment and bag strip occurred no later than this time.

Based on the time to line stretch and the suspension line plus attachment system length, the average velocity provided by the mortar in deploying the parachute out to line stretch was 36 m/s (117 ft/s).

Inflation.- Selected frames from the aft camera film showing the initial canopy inflation, unsteady reefed inflation, steady reefed inflation, the disreefing sequence, and steady unreefed inflation are presented in figure 17.

A time history of the ratio of the instantaneous parachute projected area to the steady unreefed area was obtained from the aft camera film and is presented in the upper part of figure 18. (A Mach number scale is also shown on the abscissa.) Parachute inflation began shortly after line stretch and the projected area increased smoothly until

0.76 second, at which time the disk part of the canopy was filled. However, the band did not open out at this time. For the next several seconds the parachute exhibited an inflation instability characterized by irregular changes in its projected area. Most of the area fluctuations were in the band, whereas the disk remained nearly fully inflated. However, the magnitudes of the fluctuations were less than those experienced during the flight test of the unreefed parachute of reference 5. At approximately 5 seconds after mortar firing, the entire parachute achieved a steady reefed inflated shape. The Mach number was 1.5 at that time and the steady projected area was 49 percent of the final unreefed, steady area.

The failure of a parachute to achieve steady inflation above a certain supersonic velocity is common to most parachute types and has been experienced previously in both wind-tunnel and flight tests of disk-gap-band parachutes. (See refs. 3 and 5.) For most types of parachutes, Mach number and porosity appear to be the most important parameters affecting inflation stability. (See ref. 8.) It is believed that distribution of porosity also must have an important effect on inflation. As seen from table I, the DGB for this test had 0.5-percent geometric porosity in the vent and 12 percent in the gap. Inflation of a DGB most likely proceeds in the following manner: A high-pressure region builds up in the crown area of the canopy where the geometric porosity is low. The incoming mass flow is relatively high; there is a little mass flow out through the vent and canopy cloth pores, but the remaining air mass flow goes toward filling the canopy disk. The disk inflates rapidly until it is completely filled. However, further inflation of the total parachute becomes hampered by the presence of the gap which provides a large area for the incoming air to exit. If the Mach number is high enough, the effect of air compressibility can be that all incoming mass flow exits immediately. Hence, the pressure buildup within the disk is not able to "jump the gap" to inflate the band. No large pressure gradient exists across the band; the band reacts to local, unsteady pressures by changing its shape in a seemingly random manner. Not until the Mach number is lowered to such a value that there will be a net mass accumulation within the enclosed volume will inflation continue toward completion. At full inflation, a detached near-normal shock will stand in front of the parachute and a high-pressure region will fill most of the canopy and hold the band out. Based on flight data for the disk-gap-band configuration, it appears that this condition exists at a Mach number of about 1.5 and below.

Disreefing occurred at 8.49 seconds and at a Mach number of 0.99. The parachute quickly filled in a steady, symmetric manner as evidenced by figures 17(d) and 18. With the exception of a few minor breathing cycles, the parachute maintained a steady inflated shape for the remainder of the flight test. It was observed on the aft camera film that the two valleys in the projected area curve at about 12 seconds and 18 seconds were due to one side of the canopy being forced inward. These valleys correspond to the occurrence of pitch and yaw peaks in figure 15. Thus, canopy distortion appears to result when the

parachute reaches a high angle of attack so that the free-stream dynamic pressure is felt on the outer surface of one side of the canopy.

Drag.- The axial-force coefficient, during the deceleration part of the test, is presented in the lower half of figure 18 as a function of time from mortar firing. The axial-force coefficient was calculated by the following equation:

$$C_{A,o} = -\frac{mga_x}{q_\infty S_o}$$

Payload drag was assumed to be small compared with parachute drag and therefore was neglected in the calculation. Also, since the accelerometers were located near the payload center of gravity, incremental accelerations from pitch and yaw were so small that the longitudinal accelerometer data could be used directly for the linear acceleration term in the equation. The 75 g-unit accelerometer was used for the first 6 seconds of calculations and the 5 g-unit accelerometer was used thereafter (with the exception of the disreef spike).

In general, the axial-force coefficient shows the same trend as the projected area history. However, for the first 5 seconds, the axial-force coefficient exhibited large variations at a frequency higher than the area variations. These variations were due to the varying parachute drag which excited the elastic system and caused it to oscillate at its natural frequency. This oscillation was felt by the payload and, as a result directly affected the axial-force-coefficient calculation through the payload acceleration term. Once the projected area became steady at a Mach number of approximately 1.5, the oscillation quickly damped out and the axial-force coefficient steadied. It remained steady until disreef. A momentary drop in the axial-force coefficient occurred when the reefing line was cut and the loading in the suspension lines was relaxed. The parachute quickly inflated. A short time (0.08 second) later the tension in the suspension lines peaked. The resulting force coefficient was about twice as large as the subsequent steady coefficient. (This large overload is not surprising if one views the disreefing and subsequent inflation as a transient forcing function on a two-body spring mass system. An analysis of this kind was performed in reference 9, where it was found that overloads as high as twice the steady load could result when the parachute filling time was very short.) After the transient effects due to the overload diminished (at about 9.5 seconds), the axial-force coefficient became fairly steady. The slight dips at 12 and 18 seconds correspond to the drop in parachute projected area mentioned previously. For the reefed data, the estimated uncertainty in $C_{A,o}$ is about ± 0.02 for both the unsteady and steady parts; for the unreefed data, the uncertainty ranges from ± 0.04 at disreef to ± 0.09 at 20 seconds.

The vertical descent velocity and effective drag coefficient based on this velocity are presented in figure 19 as a function of altitude. The effective drag coefficient was calculated by the following equation:

$$(C_{D,o})_{eff} = \frac{2m}{\rho_\infty \dot{Z}_E^2 S_o}(g - \ddot{Z}_E)$$

During descent from 45.7 km (150 000 ft) to 9.1 km (30 000 ft), the effective drag coefficient was fairly constant and had an average value of 0.57. The estimated uncertainty is ±0.04 based on a 3-percent density error and a 5-percent velocity error. This value was the highest value of effective drag coefficient yet achieved with a large size DGB. (See refs. 2, 4, and 5.) But this test was the only one in the series in which there was both no canopy damage and no shrinkage of parachute tapes due to heat sterilization.

Average values of axial-force coefficient and effective drag coefficient were determined for Mach number increments of 0.1 and the results are presented in figure 20 as the drag coefficient. It is assumed, of course, that the effects of suspension-line elasticity can be negated by the averaging process on $C_{A,o}$ to yield the net drag efficiency of the parachute at each Mach number increment. From figure 20, it can be seen that the drag coefficient during the unsteady, reefed part of the test, above $M = 1.9$, was 0.15. This value is the same as that obtained for a 1.7-meter (5.5-ft) DGB with the same amount of reefing and at a steady Mach number of 2.0 in the wind-tunnel test of reference 3. Between $M = 1.9$ and $M = 1.5$ (which was a flight time increment of only 1.9 seconds), the unsteadiness diminished. During steady reefed operation below $M = 1.5$, the drag coefficient was 0.30. For the unreefed data of figure 20, both the $C_{A,o}$ values and the $(C_{D,o})_{eff}$ values have averages between 0.56 and 0.57.

Stability.- The attitude history of the payload during the 20-second deceleration period after mortar firing was discussed earlier with the data presented in figures 15 and 16. During the descent portion of the flight test from an altitude of 46.3 km (152 000 ft) to an altitude of 18.6 km (61 000 ft), the gyro patform data were transformed to the earth-fixed Euler angle system shown in figure 21 by the method presented in an appendix to reference 7. The resulting data are presented in figure 22. It can be seen from the figure that both pitch and yaw show a long period oscillation (in the range from 5 to 10 seconds) with a superimposed short-period oscillation (about 1 second) at times. Both figures 15 (the unreefed data) and 22 show similar short-period, low-amplitude oscillations for the payload.

Since no large-amplitude, long-period oscillations are evident from the film data once steady unreefed inflation is achieved, it is believed that the large pitch and yaw motions shown in figure 22 result from the payload parachute system acting together like a rigid body. The high-frequency, small-amplitude pitch and yaw motions result from the payload itself oscillating about the parachute axis of symmetry. It appears from the data that the payload-parachute system motion is generally planar, the plane of oscillation varying and having little, if any, coning. Planar oscillations can be induced by wind shear;

however, it is difficult to discern a direct correlation between figures 10 and 22. In any case, the payload-parachute system displayed good stability. The resultant angles $|\delta_E|$ average about 10^o above 33.5 km (110 000 ft) and about 5^o below this altitude.

Postflight parachute inspection.- The parachute system was not damaged during the flight test. In addition, there was no evidence of structural degradation from aerodynamic heating. A photograph of the descending parachute shortly before impact is presented in figure 23.

CONCLUSIONS

A reefed 12.2-meter nominal-diameter (40-ft) disk-gap-band parachute was deployed from an instrumented payload at an altitude of 43.6 km (143 000 ft), a Mach number of 2.58, and a dynamic pressure of 972 N/m^2 (20.3 lb/ft^2). The parachute was disreefed when the Mach number had decreased to 0.99 and the dynamic pressure to 81 N/m^2 (1.7 lb/ft^2). Based on an analysis of the data, the parachute performed effectively and provided good drag and stability for both the reefed and unreefed parts of the test. Specifically, it is concluded that

1. The mortar properly ejected the parachute from the payload and full-length deployment of the parachute canopy occurred before 0.62 second.

2. The disk section of the canopy was inflated by 0.76 second; however, the band did not achieve a stable inflated shape until 5 seconds after mortar firing when the Mach number had decreased to 1.5. The magnitudes of the area fluctuations were less severe than those experienced previously for an unreefed parachute.

3. Disreefing occurred 8.49 seconds after mortar firing and a full inflation was achieved 0.17 second later. With the exception of a few minor breathing cycles initially, the parachute maintained a fully inflated shape for the remainder of the flight test.

4. The initial parachute opening load relative to free-stream dynamic pressure was small (22 107 N (4970 lb)) because of reefing. The maximum disreef load was about twice as high as the steady drag load would be at the same free-stream dynamic pressure.

5. The average axial-force coefficient of the reefed parachute during supersonic flight varied from 0.15 during unsteady inflation to 0.30 at steady inflation. The average axial-force coefficient of the unreefed parachute during subsonic flight and the effective drag coefficient during descent were approximately 0.57.

6. During descent, payload-parachute system motions were generally planar and averaged about 10^o above 33.5 km (110 000 ft) and about 5^o below this altitude.

7. The parachute was not damaged during flight and there was no evidence of structural degradation from aerodynamic heating.

Langley Research Center,
National Aeronautics and Space Administration,
Hampton, Va., August 10, 1971.

APPENDIX A

A PREVIOUS TEST OF A REEFED DISK-GAP-BAND PARACHUTE

A 12.2-meter (40-ft) nominal diameter disk-gap-band parachute was flight tested on December 16, 1969, at White Sands Missile Range. This was the first test in the PEPP and SHAPE series of a reefed parachute. The test parachute deployed properly from the payload, but the reefing system tore loose from the parachute canopy immediately after inflation of the canopy disk. The canopy cloth became torn, the tears propagated, and heavy damage resulted. However, enough drag was provided so that the two ribbon recovery parachutes did not have to be deployed to save the payload from a damaging ground impact.

Test Parachute Description

The test parachute was similar to the one described in this paper with the following exceptions:

(1) This parachute did not incorporate the gap reinforcement and rip-stop tapes shown in figure 3.

(2) The dacron canopy cloth was type 55, regular tenacity, 70 denier with a measured tensile strength of 119 N/cm (68 lb/in.) in both the warp and fill direction.

(3) The reefing rings were attached to only the disk hem tape on the inside surface of the canopy. Part of the reefing system is shown in figure 24. This system should be compared with the method of attaching rings depicted in figure 5 of this paper.

Performance Analysis

Mortar firing to initiate parachute deployment occurred when the payload was at a Mach number of 2.77 and an altitude of 43.6 km (143 000 ft); the dynamic pressure was 958 N/m^2 (20.0 lb/ft^2). A time history of the longitudinal accelerometer is presented in figure 25 for a 5-second period after mortar firing. For about the first second, the longitudinal accelerations are typical for the mortar deployment method used: 7.3 g-units at 0.17 second from full-length deployment of the bridle and risers; 6.8 g-units snatch force at 0.45 second due to suspension-line stretch; 25.6 g-units opening load at 0.95 second associated with reefed inflation. After 1 second, however, acceleration levels were relatively low; this condition would indicate low drag.

Selected frames from the onboard camera are presented in figure 26. Figure 26(a) shows part of the inflation process beginning with line stretch and ending with first full inflation of the parachute disk. Figure 26(b) begins with the first frame where there is

evidence of reefing system failure and ends with a frame showing actual loss of canopy material. It is evident from this how quickly the initial damage propagated. Figure 26(c) gives some indication of the parachute damage incurred by 2 seconds.

A postflight analysis was made of all available data, and tensile tests of parachute specimens with ring attachments were performed. Figure 27 presents photographs of a specimen which had been subjected to tension until partial failure resulted. Figure 27(a) shows the disk hem and cloth pulled loose from the radial tape and figure 27(b) shows the disk hem starting to tear loose from the disk canopy cloth. As a result, it has been concluded that immediately after inflation of the canopy disk, the tension in the reefing line caused the disk hem to tear loose from the radial tapes and canopy cloth in the region of the reefing ring attachment. The failure can be attributed to the fact that the reefing rings were attached to the disk hem only. Thus, the tension in the reefing line resulted in an inward force on the disk hem, whereas the inflating parachute placed an outward force on the radial tapes and parachute cloth. Once torn, the tears easily propagated up the gores toward the vent. The disk sustained major damage; the band suffered minor damage along the upper edge.

APPENDIX B

PARACHUTE PACKING PROCEDURE

Before flight the test parachute was stretched out on packing tables with a 445-N (100-lb) tension applied to the suspension-line—radial-tape system. The reefing-line cutters and the reefing line were installed. The radial tapes were arranged into four stacks of eight tapes each along the center of the tables, and the cloth portion of the canopy gores were pleated into two stacks of 16 gores each. The canopy cloth stacks were separated by the radial tape stacks. Figure 28(a) shows the parachute at this stage of the packing. The canopy cloth stacks were then "S" folded (one stack over and the other stack under the radial tapes) to achieve a folded canopy width of about 30 cm (12 in.). The bottom of the band and edge of the disk, after S folding, are shown in figures 28(b) and 28(c), respectively. A reefing-line cutter and part of the reefing line are visible in figure 28(c).

The parachute deployment bag was a cylindrical container, fabricated of dacron canvas, lined with teflon fabric, and split longitudinally on each side. The bag was permanently attached to the parachute at six locations equally spaced around the periphery of the vent. Each of the six independent attachments consisted of three progressively larger and stronger loops of nylon cord, the largest of which was 39 cm long (12 in.) with a tensile strength of 175 N (780 lb). Figure 28(d) shows the deployment bag attachment.

The attached deployment bag was temporarily placed in a cylindrical packing fixture. Starting with the crown, all the disk section of the canopy was accordion-folded into the bag. This accordion fold is shown in figure 28(e). The top of the band was placed proximate to the edge of the disk and the mechanical actuators (lanyards) of the reefing-line cutters were secured to beckets located at the top of the band. (This arrangement was made so that on deployment, the separation of the band from the disk would activate the reefing cutter delay train.) The band part of the canopy was then accordion-folded into the bag and the complete canopy was forced down into the bag by applying a force of 66 800 N (15 000 lb) with a hydraulic press.

Next, the suspension lines were accordion-folded into the bag in layers. Figure 28(f) shows the first layer being placed in the bag. The total length of the suspension lines and part of the riser were placed in the bag and the force of 66 800 N (15 000 lb) was reapplied. The packed parachute, after the packing force was removed, is shown in figure 28(g).

The parachute pack was then removed from the packing fixture. Figure 28(h) shows the parachute at this stage. A temporary lacing is shown on the bag in the figure. This lacing was put on the bag prior to its placement in the packing fixture.

The bag mouth was then tied closed with a loop of 2670 N (600 lb) (specified strength) braided dacron cord which passed through a circular knife attached to the parachute riser. Next, the bag was re-laced with a 2670-N (600-lb) (specified strength) braided dacron cord which laced from the bottom of one side of the bag to the top of that side, across the mouth and through the circular knife, and then laced down the other side of the bag.

The packed parachute was placed in the payload mortar tube with the mouth end of the bag in the sabot or breech end of the mortar. That part of the riser which was outside of the bag was placed along the side of the bag and exited the mortar tube at the aft end of payload. The free end of that riser was then coupled to the parachute attachment system (swivel, intermediate riser, tensiometer, and bridle), all of which were stowed in the payload around the outside of the mortar. Figure 28(i) is a photograph of the aft end of the payload with the packed parachute in place. This figure shows the three bridle attachment points and the mortar cover which held the packed parachute in place. Felt disks (filler material) were sandwiched between the deployment bag and the mortar cover to achieve a tight longitudinal fit of the packed parachute in the mortar tube. The mortar cover was permanently attached to the deployment bag by inserting beckets attached to the bag through slots in the cover and then looping cord through the beckets as shown in figure 28(i).

REFERENCES

1. Murrow, Harold N.; and McFall, John C., Jr.: Some Test Results From the NASA Planetary Entry Parachute Program. J. Spacecraft Rockets, vol. 6, no. 5, May 1969, pp. 621-623.

2. Whitlock, Charles H.; and Bendura, Richard J.: Inflation and Performance of Three Parachute Configurations From Supersonic Flight Tests in a Low-Density Environment. NASA TN D-5296, 1969.

3. Bobbitt, P. J.; Mayhue, R. J.; Faurote, G. L.; and Galigher, L. L.: Supersonic and Subsonic Wind-Tunnel Tests of Reefed and Unreefed Disk-Gap-Band Parachutes. AIAA Paper No. 70-1172, Sept. 1970.

4. Eckstrom, Clinton V.: Flight Test of a 40-Foot-Nominal-Diameter Disk-Gap-Band Parachute Deployed at a Mach Number of 3.31 and a Dynamic Pressure of 10.6 Pounds Per Square Foot. NASA TM X-1924, 1970.

5. Eckstrom, Clinton V.; and Preisser, John S.: Flight Test of a 40-Foot-Nominal-Diameter Disk-Gap-Band Parachute Deployed at a Mach Number of 2.72 and a Dynamic Pressure of 9.7 Pounds Per Square Foot. NASA TM X-1623, 1968.

6. Anon.: U.S. Standard Atmosphere, 1962. NASA, U.S. Air Force, and U.S. Weather Bureau, Dec. 1962.

7. Preisser, John S.; and Eckstrom, Clinton V.: Flight Test of a 30-Foot-Nominal-Diameter Cross Parachute Deployed at a Mach Number of 1.57 and a Dynamic Pressure of 9.7 Pounds Per Square Foot. NASA TM X-1542, 1968.

8. Amer. Power Jet Co.: Performance of and Design Criteria for Deployable Aerodynamic Decelerators. ASD-TR-61-579, U.S. Air Force, Dec. 1963. (Available from DDC as AD 429 971.)

9. Preisser, John S.; and Greene, George C.: Effect of Suspension Line Elasticity on Parachute Loads. J. Spacecraft Rockets, vol. 7, no. 10, Oct. 1970, pp. 1278-1280.

TABLE I.- GEOMETRIC CHARACTERISTICS

Parachute type	Disk gap band
Number of gores and suspension lines	32
Nominal diameter, D_o	12.2 m (40 ft)
Constructed diameter	8.87 m (29.11 ft)
Nominal area, S_o	116.7 m^2 (1256 ft^2)
Disk area (including vent area)	61.8 m^2 (665 ft^2)
Disk area, percent of S_o	53
Vent area	0.58 m^2 (6.28 ft^2)
Vent area, percent of S_o	0.5
Gap area	14.0 m^2 (151 ft^2)
Gap area, percent of S_o	12
Band area	40.9 m^2 (440 ft^2)
Band area, percent of S_o	35
Total gap and vent areas (geometric porosity), percent of S_o	12.5
Constructed and theoretical gore width at top and bottom of band, outer edge of disk	0.87 m (2.86 ft)
Constructed gore width at vent	9.4 cm (3.7 in.)
Theoretical gore width at vent	8.4 cm (3.3 in.)
Fullness in gore width at vent, percent	11
Constructed and theoretical vent tape length (vent diameter)	0.86 m (2.83 ft)
Length (distance from bottom of band to confluence point) of each suspension line, measured under a tension of 44.5 N (10 lb)	12.2 m (40 ft)
Diameter of reefing line loop	3.42 m (11.2 ft)
Distance from aft end of payload to confluence point	3.44 m (11.3 ft)

TABLE II.- MATERIAL CHARACTERISTICS

Dacron canopy cloth (rip-stop weave, type 52 high tenacity – 55 denier yarn):	
Unit weight	70.5 g/m^2 (2.08 oz/yd^2)
Tensile strength (average of five measurements, ravel strip method):	
Warp direction	184 N/cm (105 lb/in.)
Fill direction	175 N/cm (100 lb/in.)
Maximum elongation (average of five measurements):	
Warp direction	32 percent
Fill direction	38 percent
Air permeability:	
$m^3/m^2/min$ at a Δp of 1.27 cm of H_2O	39.3
($ft^3/ft^2/min$ at a Δp of 0.5 in. of H_2O)	(129)
Nomex canopy cloth (plain weave, 200 denier yarn):	
Unit weight	99 g/m^2 (2.9 oz/yd^2)
Tensile strength (average of five measurements, ravel strip method):	
Warp direction	215 N/cm (123 lb/in.)
Fill direction	214 N/cm (122 lb/in.)
Maximum elongation (average of five measurements):	
Warp direction	34 percent
Fill direction	36 percent
Air permeability:	
$m^3/m^2/min$ at a Δp of 1.27 cm of H_2O	55.2
($ft^3/ft^2/min$ at a Δp of 0.5 in. of H_2O)	(181)
Radial and hem tapes (type 52, high tenacity dacron):	
Width	1.9 cm (0.75 in.)
Thickness	0.069 cm (0.027 in.)
Unit weight	8.58 g/m (0.277 oz/yd)
Maximum elongation	28 percent
Tensile strength	2589 N (582 lb)
Rip-stop and gap reinforcement tapes (type 52, high tenacity dacron):	
Width	1.9 cm (0.75 in.)
Thickness	0.069 cm (0.027 in.)
Unit weight	8.58 g/m (0.277 oz/yd)
Maximum elongation	30 percent
Tensile strength (specified minimum)	1334.4 N (300 lb)
Suspension lines (type 52, high tenacity dacron):	
Unit weight	8.30 g/m (0.268 oz/yd)
Maximum elongation	30 percent
Tensile strength	3114 N (700 lb)
Reefing line (type 52, high tenacity dacron):	
Unit weight	27.6 g/m (0.89 oz/yd)
Maximum elongation	15 percent
Tensile strength (specified minimum)	8896 N (2000 lb)
Tensile strength (actual)	11 120 N (2500 lb)
Riser webbing (MIL-W-25361A, type III dacron):	
Width, nominal	4.4 cm (1.72 in.)
Thickness, nominal	0.2 cm (0.08 in.)
Unit weight, maximum	77.5 g/m (2.5 oz/yd)
Elongation, maximum at 90 percent of specified minimum tensile strength	17.5 percent
Tensile strength (specified minimum)	31 136 N (7000 lb)
Tensile strength (actual)	36 162 N (8130 lb)

TABLE III.- PARACHUTE SYSTEM WEIGHTS

Parachute, packed, including canopy, suspension lines, riser, reefing system, and deployment bag (measured)		18.24 kg (40.2 lb)
Dacron canopy cloth (estimated)	6.22 kg (13.70 lb)	
Nomex canopy cloth (estimated)	2.81 kg (6.18 lb)	
Suspension lines (estimated)	3.33 kg (7.33 lb)	
Radial and hem tapes (estimated)	2.61 kg (5.75 lb)	
Rip-stop and gap reinforcement tape (estimated)	0.38 kg (0.84 lb)	
Riser, including links (estimated)	0.86 kg (1.90 lb)	
Reefing system (measured)	0.73 kg (1.60 lb)	
Deployment bag (measured)	0.57 kg (1.25 lb)	
Thread, ink, and other miscellaneous items (estimated)	0.75 kg (1.65 lb)	
Mortar cover and filler material (measured)		0.78 kg (1.70 lb)
Intermediate riser and swivel (measured)		1.33 kg (2.94 lb)
Total weight of system above the tensiometer (measured)		20.35 kg (44.8 lb)
Tensiometer (estimated)		0.68 kg (1.5 lb)
Bridle (estimated)		0.68 kg (1.5 lb)
Payload (estimated)		107.10 kg (235.8 lb)
Total system weight (measured)		128.81 kg (283.6 lb)

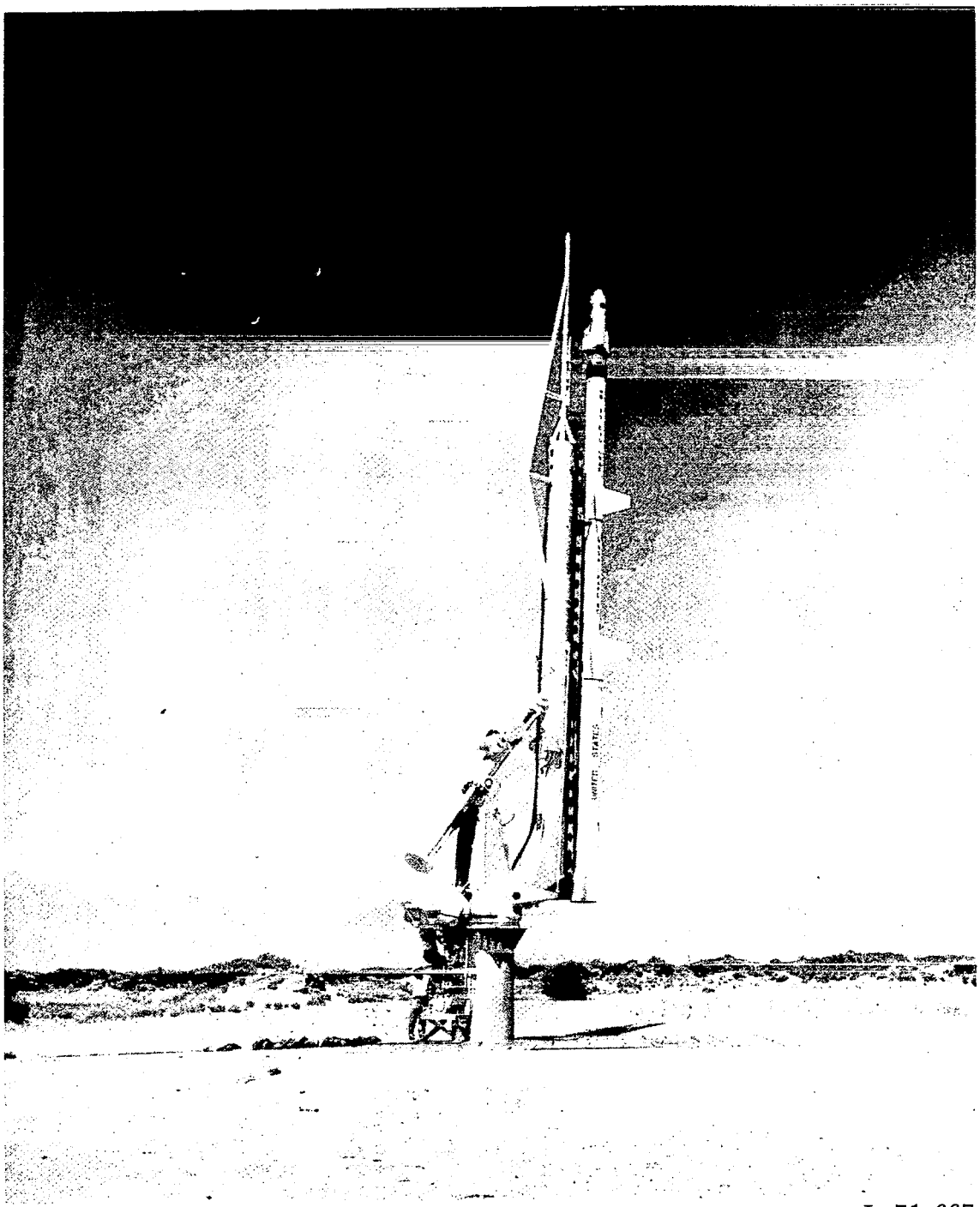

L-71-667

Figure 1.- Photograph of rocket vehicle in launch position.

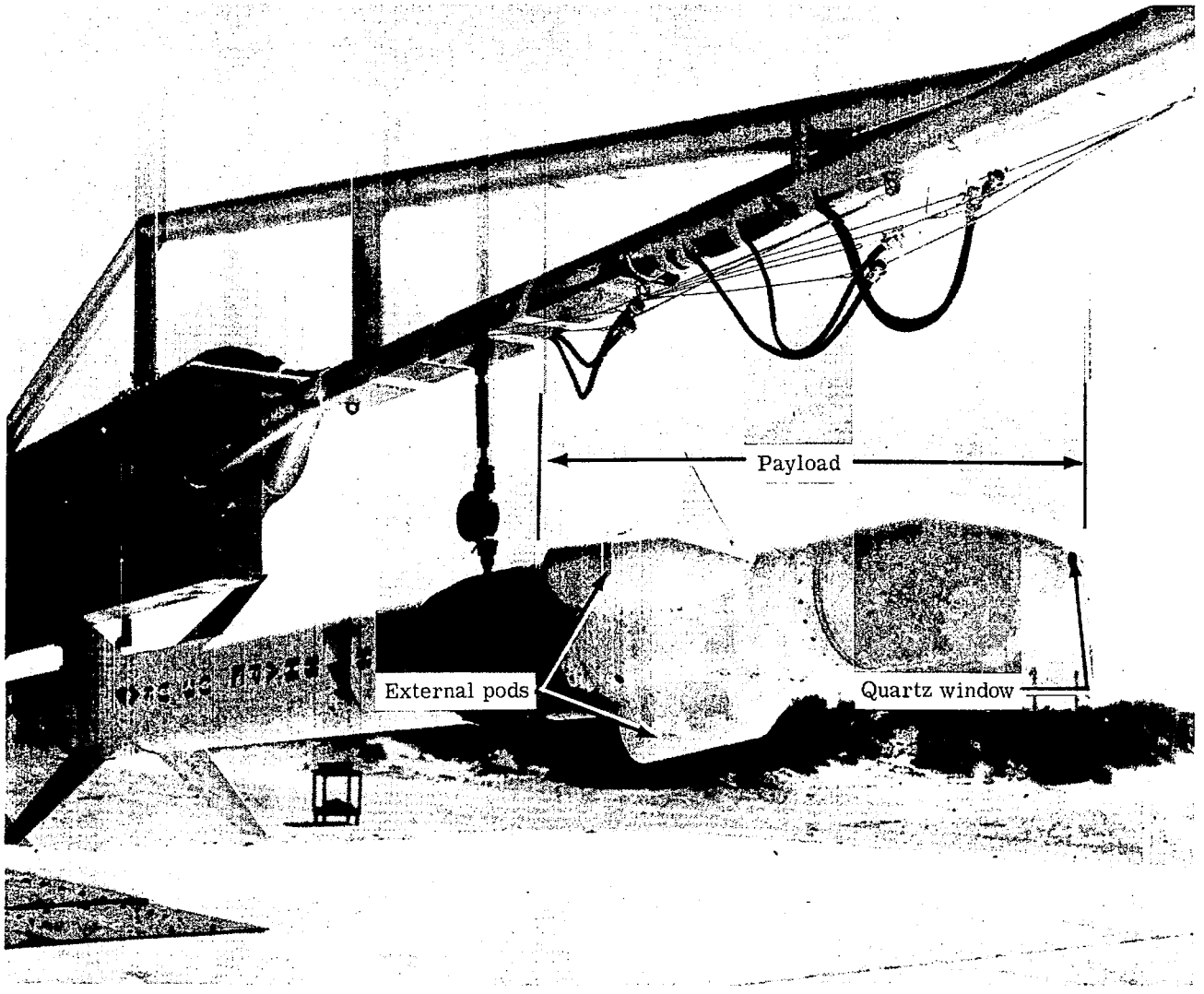

L-71-668

Figure 2.- Photograph of test payload attached to rocket vehicle.

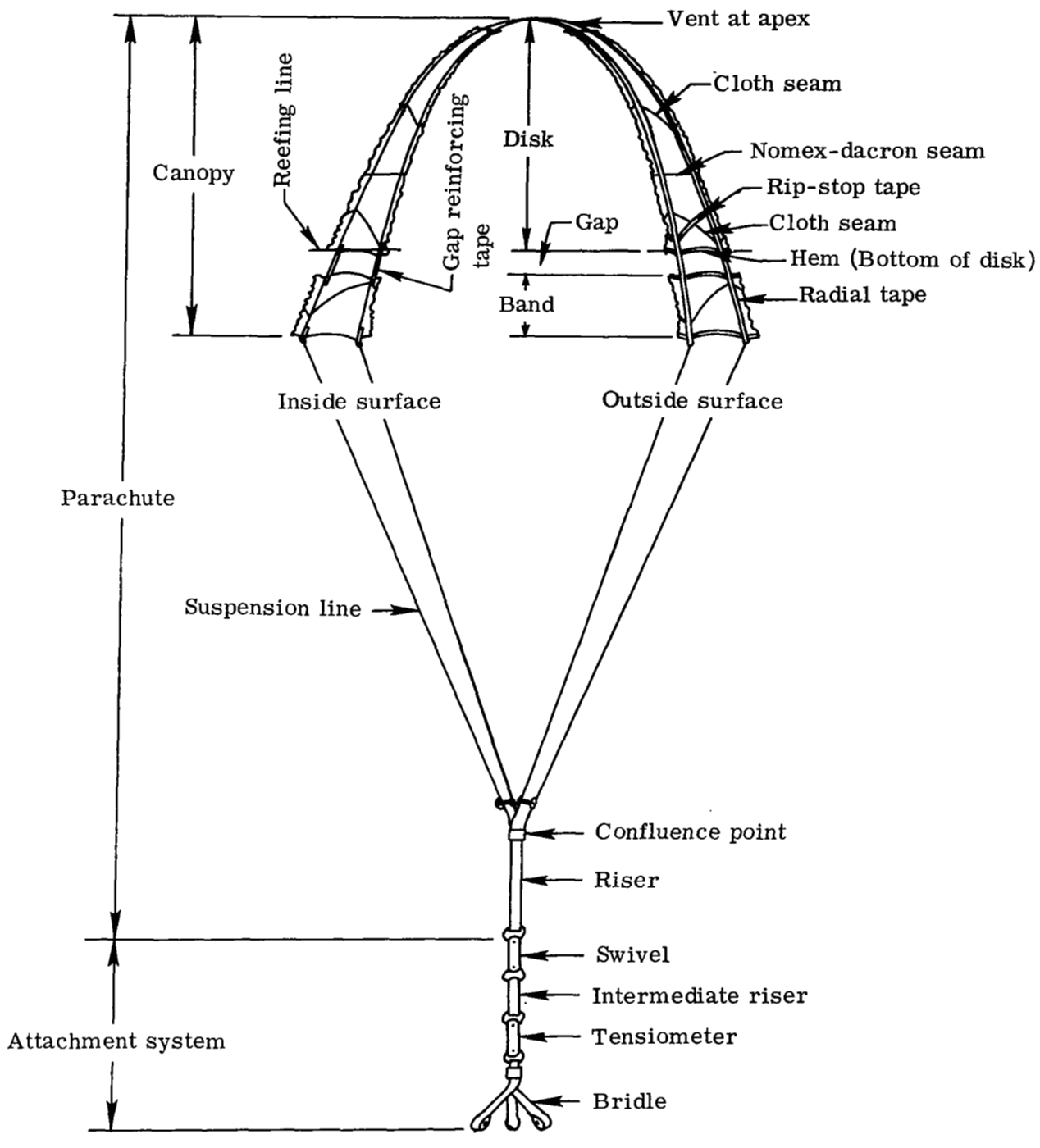

Figure 3.- Parachute and attachment system nomenclature.

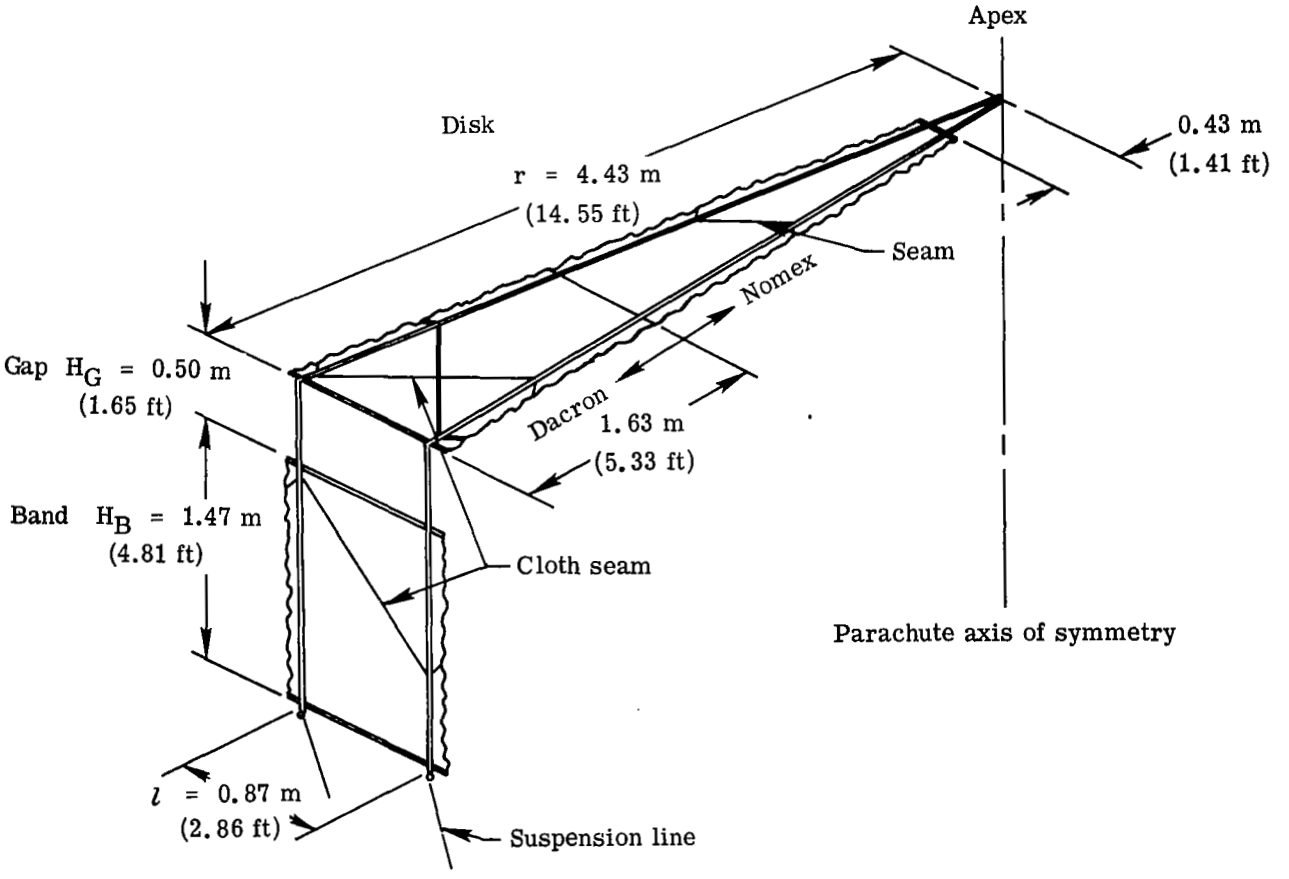

H_B height of band
H_G height of gap
r radius of circumscribed circle

Figure 4.- Principal dimensions of parachute gore.

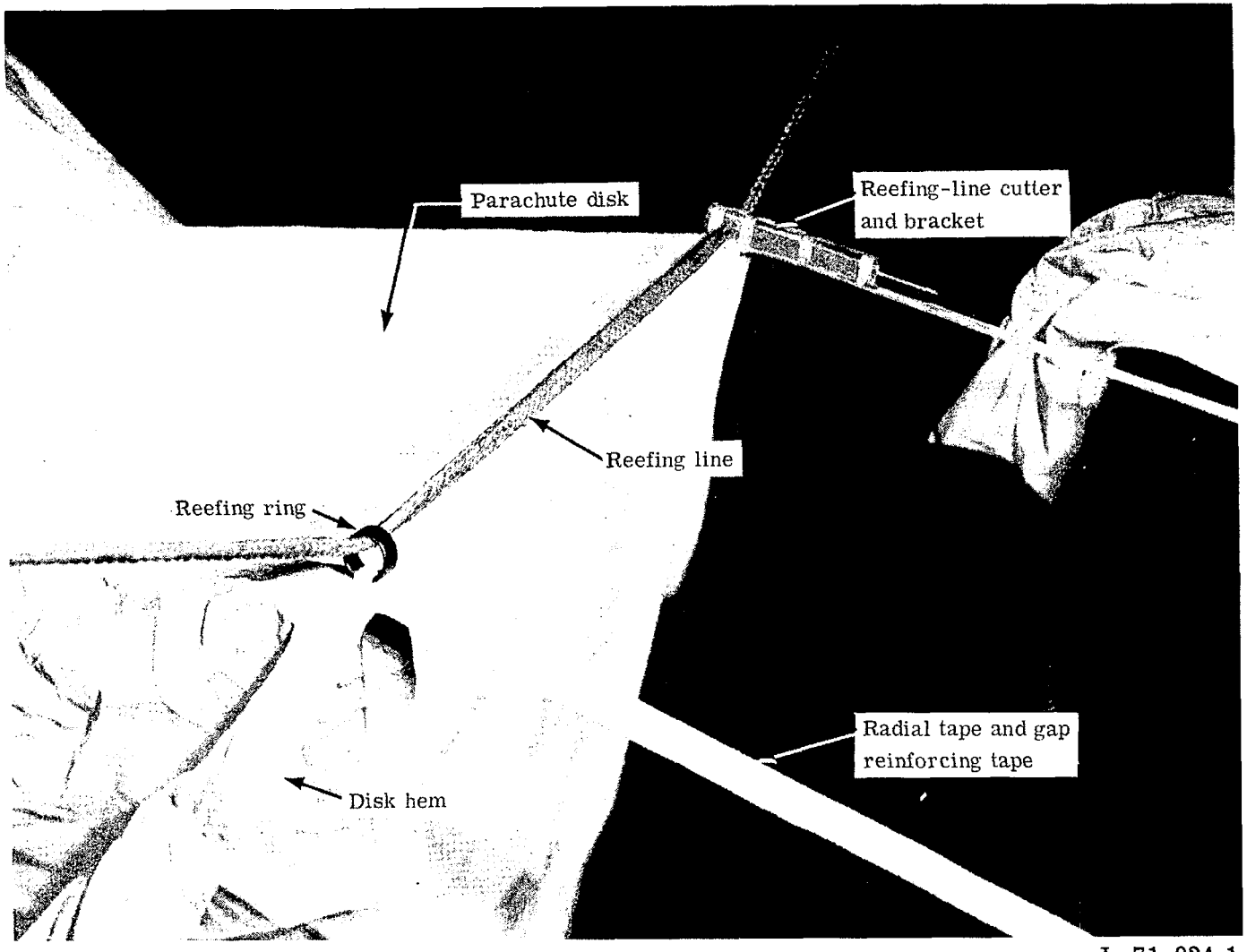

L-71-824.1

Figure 5.- Photograph of part of reefing system.

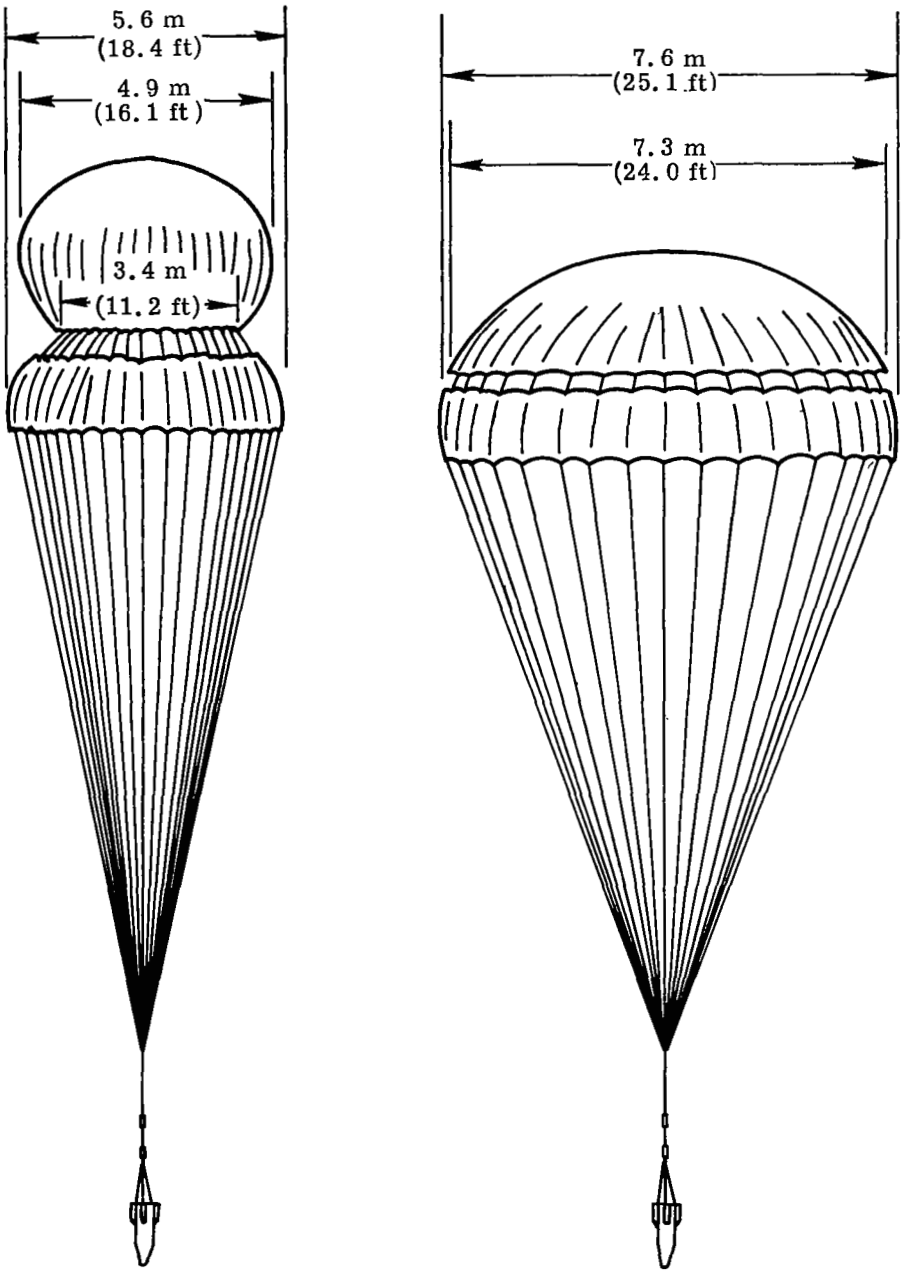

Figure 6.- Flight configuration.

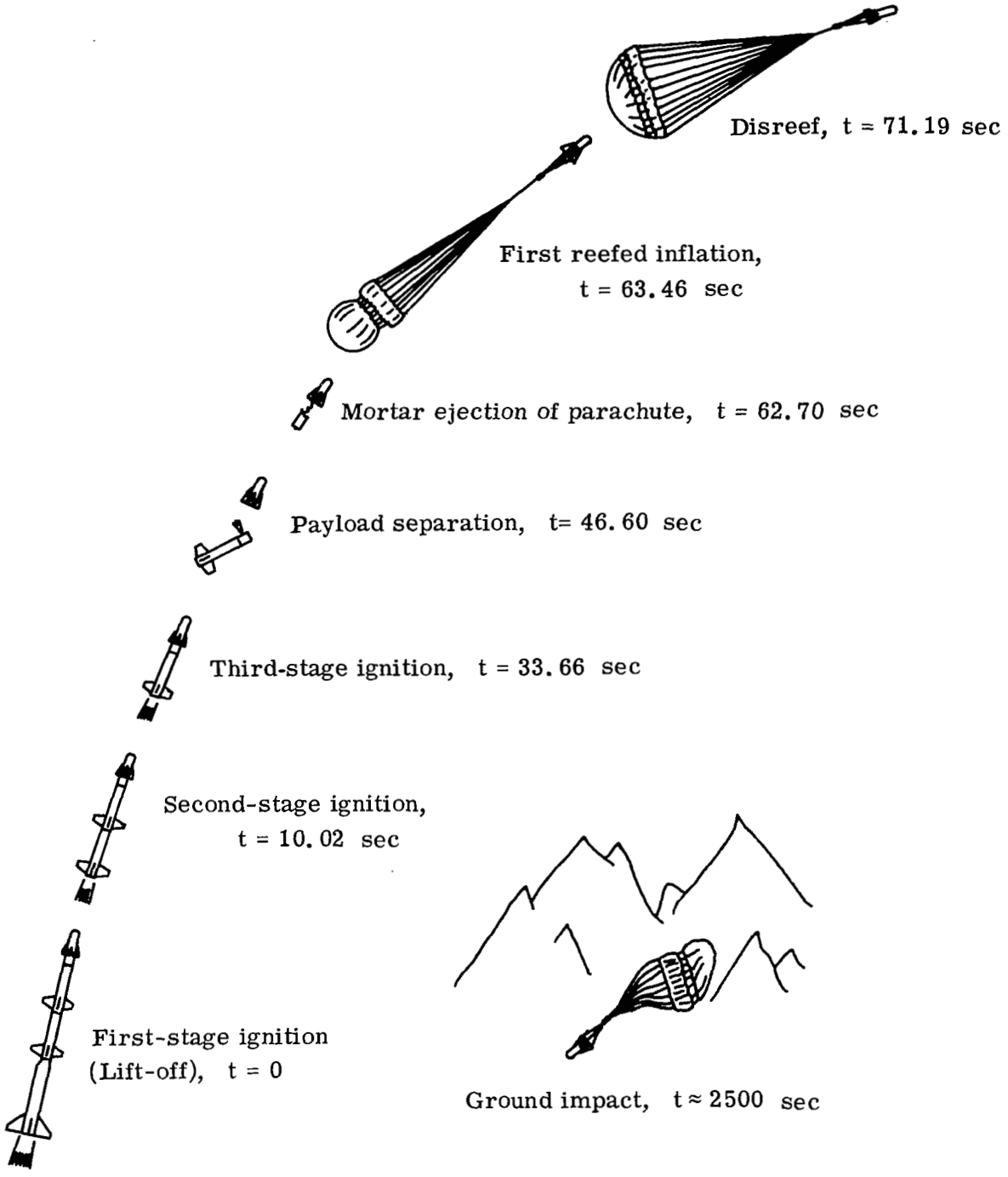

Figure 7.- Flight sequence of events.

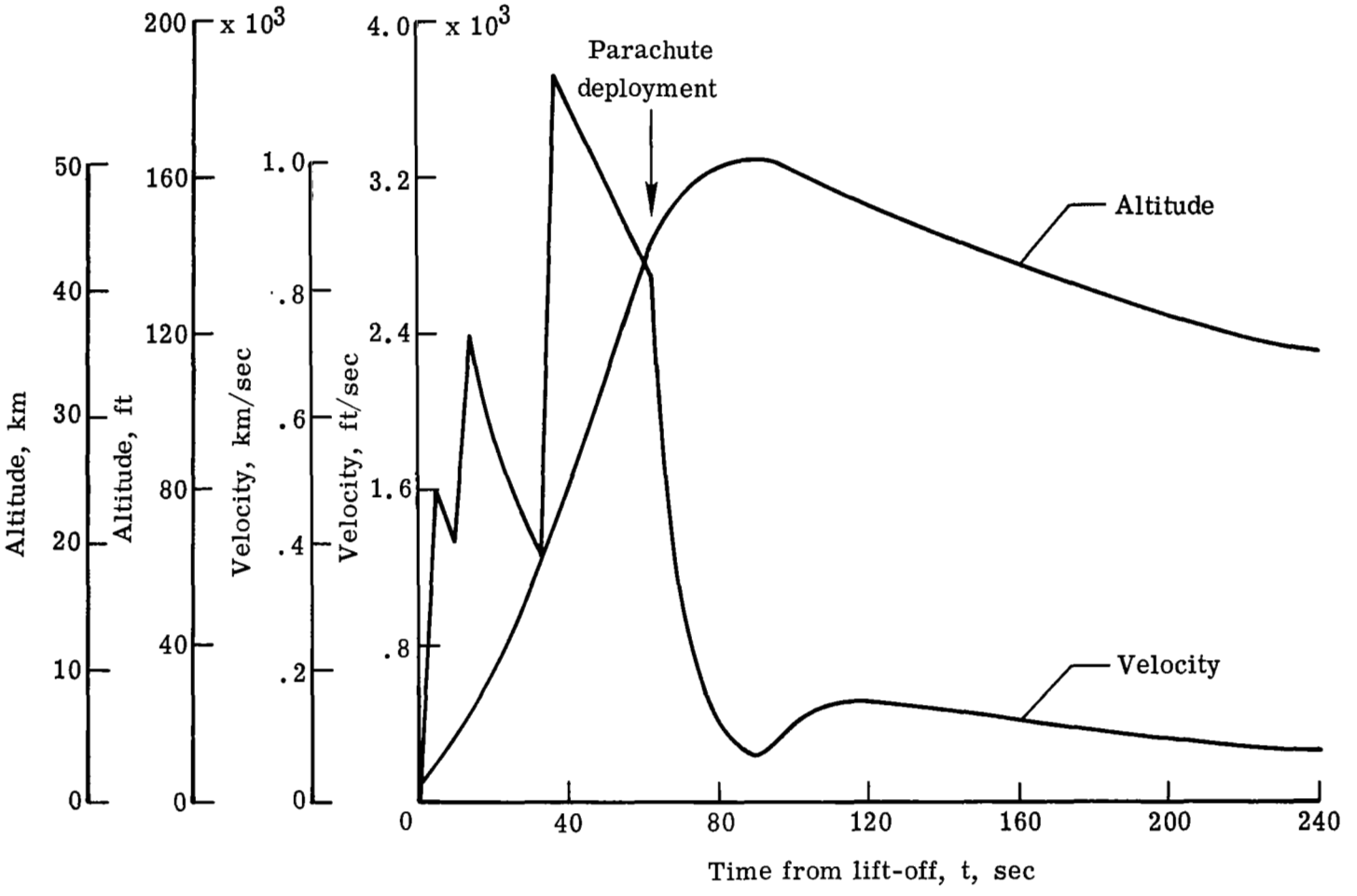

Figure 8.- Time histories of altitude and velocity.

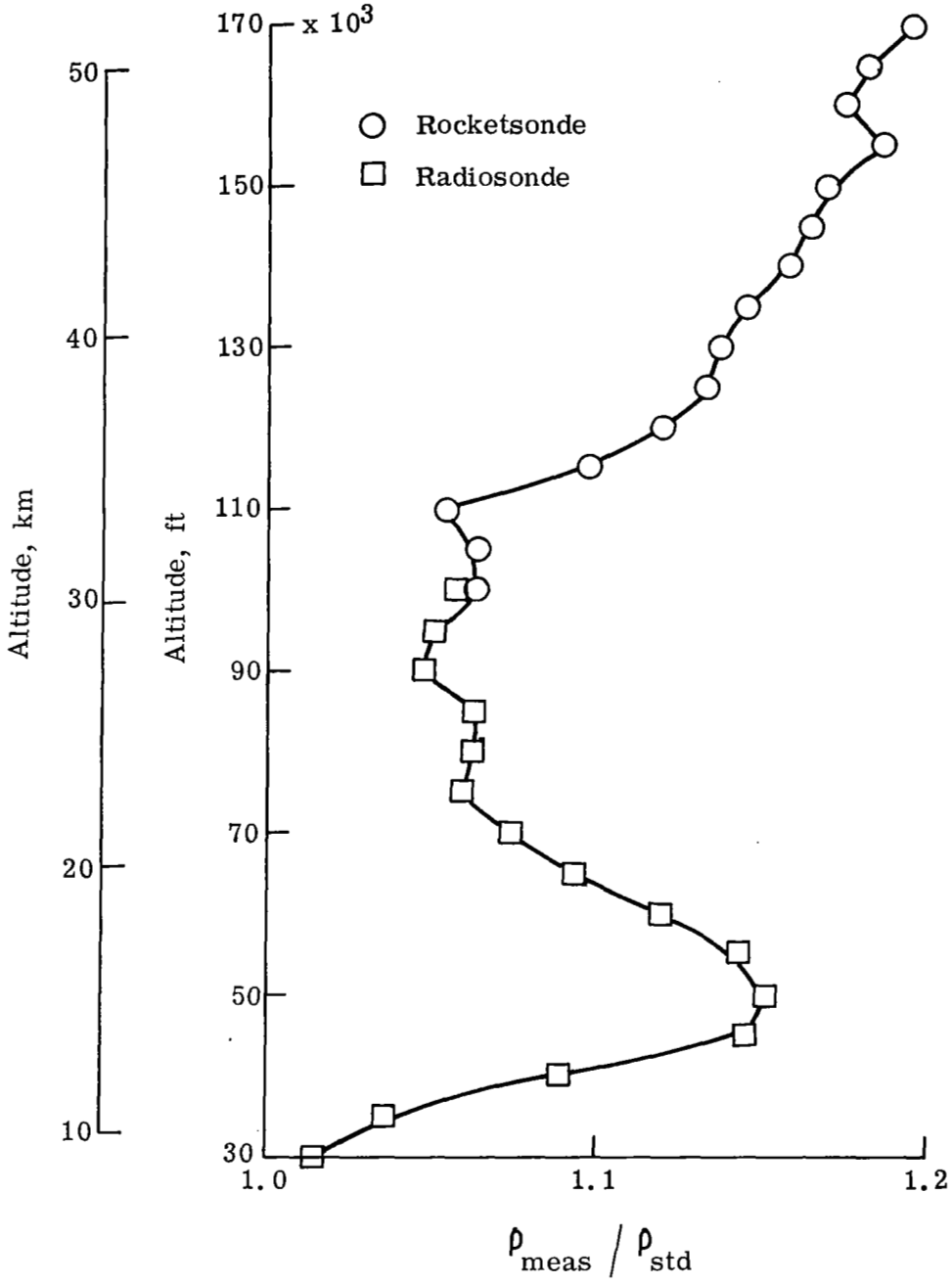

Figure 9.- Atmospheric density profile.

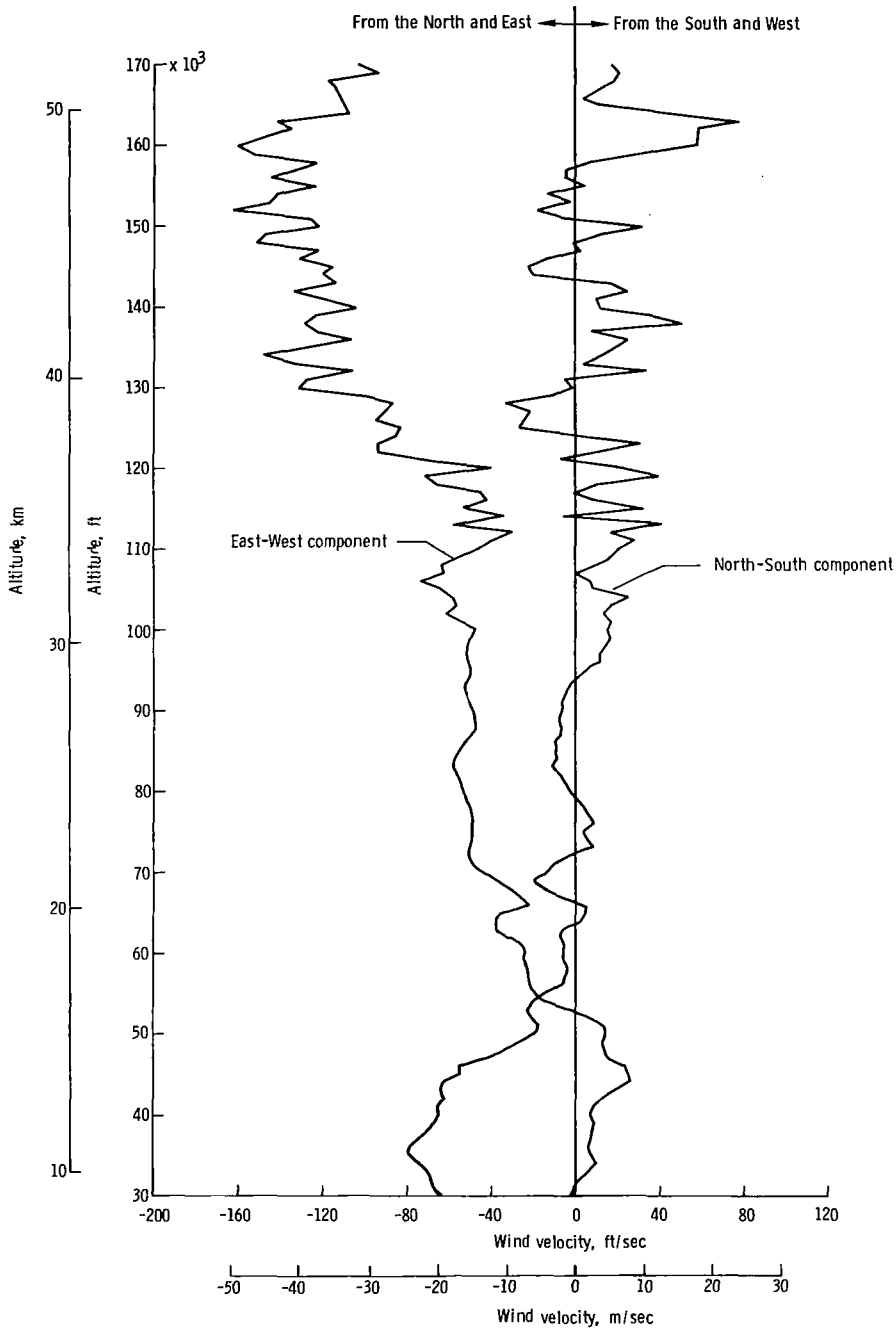

Figure 10.- Wind-velocity profile.

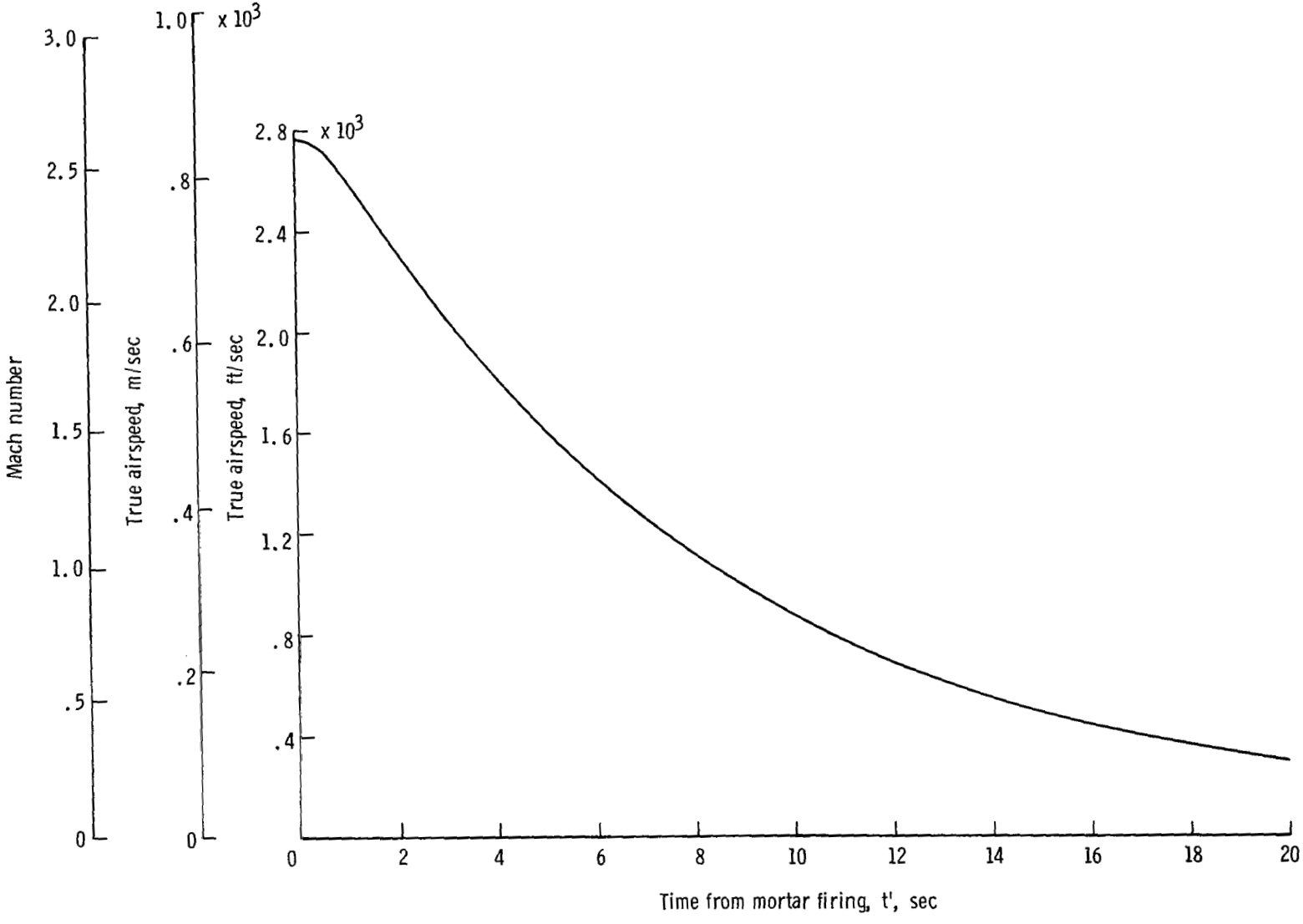

Figure 11.- Mach number and true airspeed time histories.

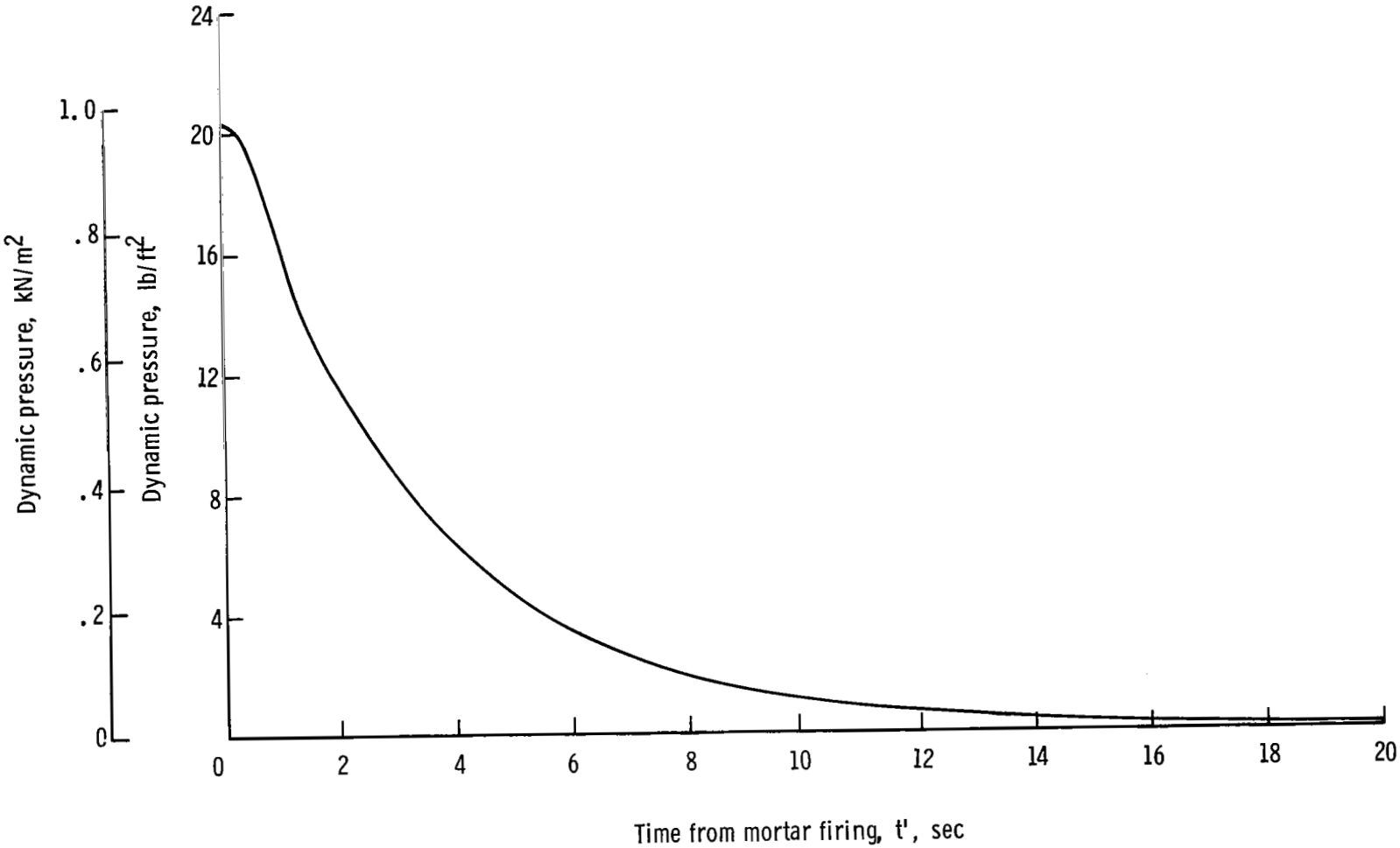

Figure 12.- Dynamic-pressure time history.

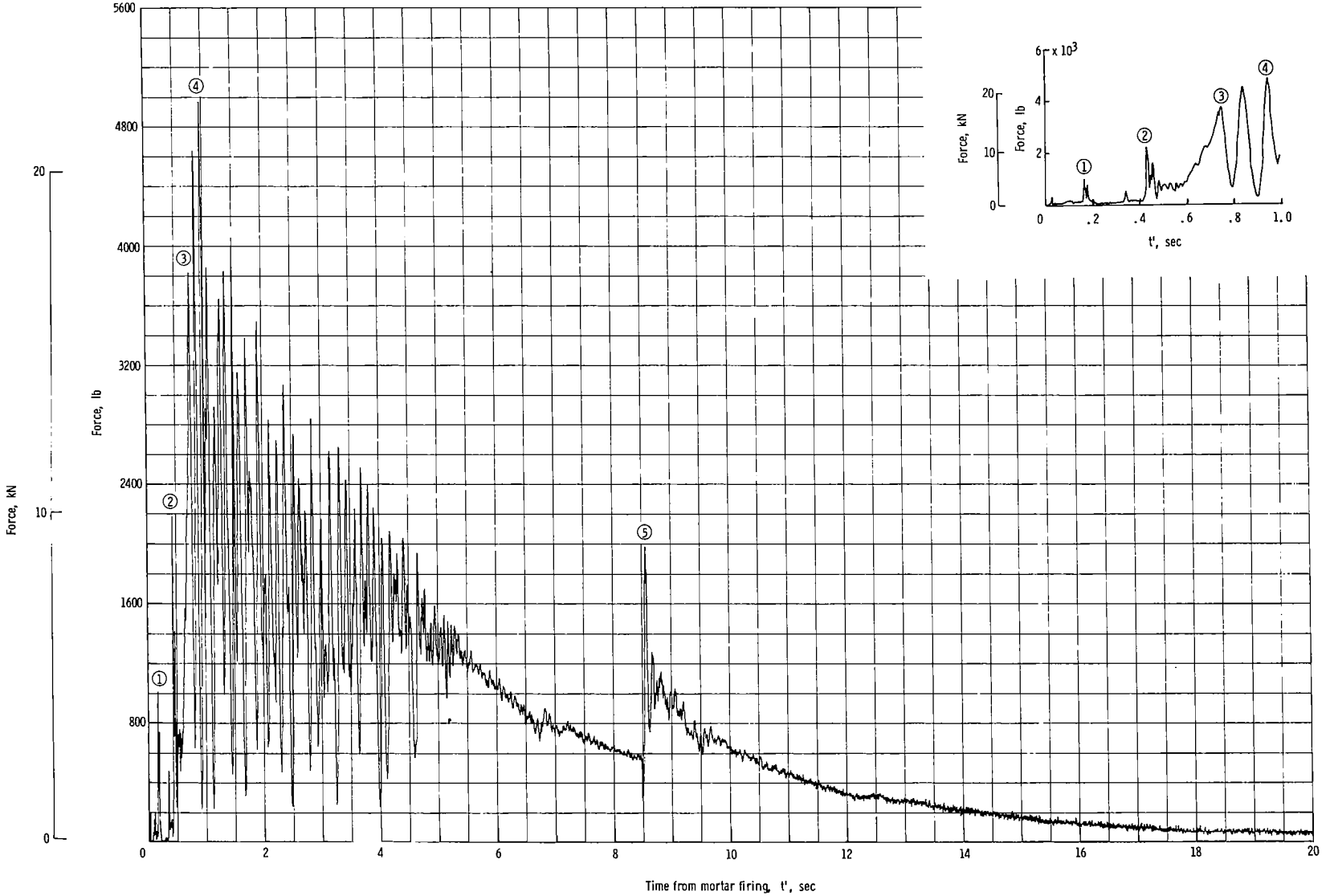

Figure 13.- Time history of force measured by tensiometer.

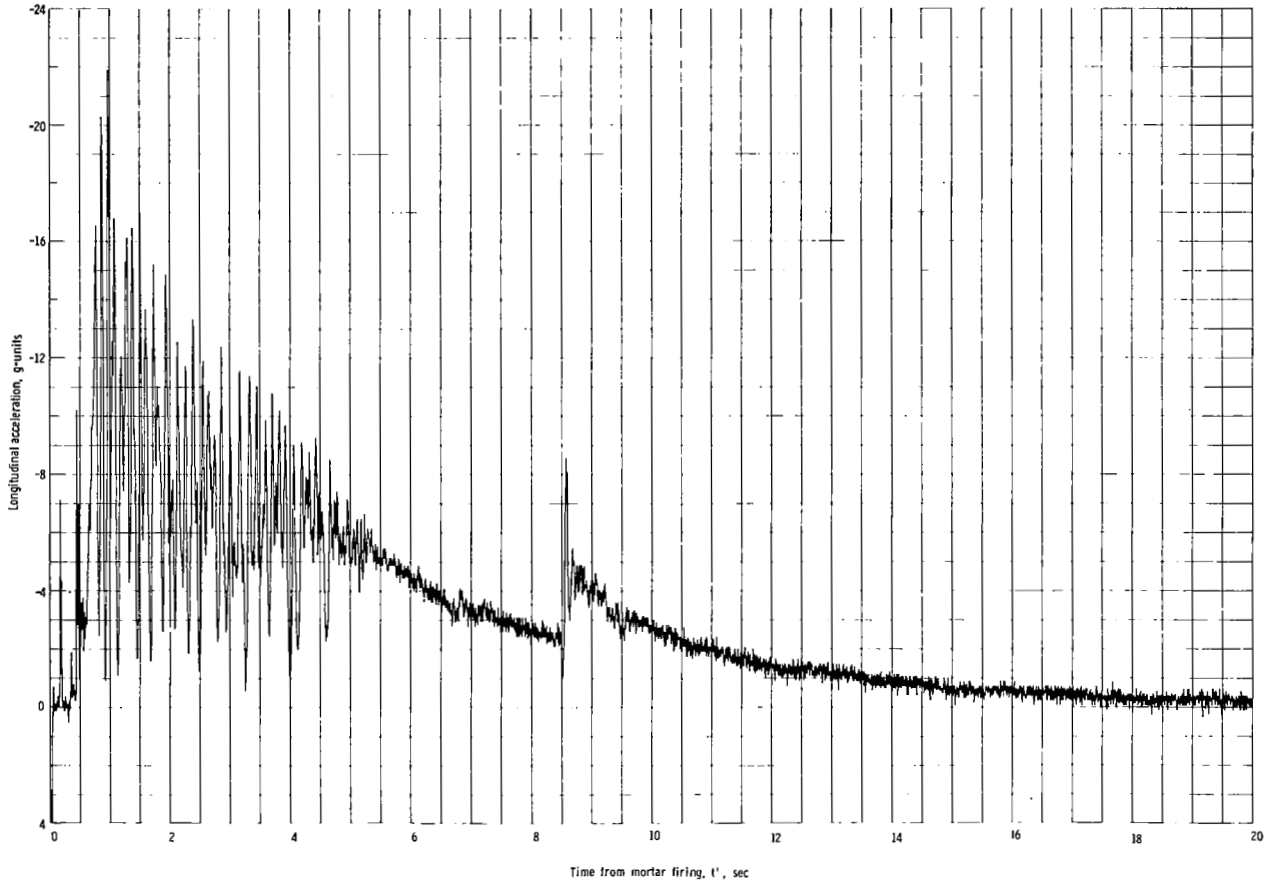

Figure 14.- Acceleration time histories.

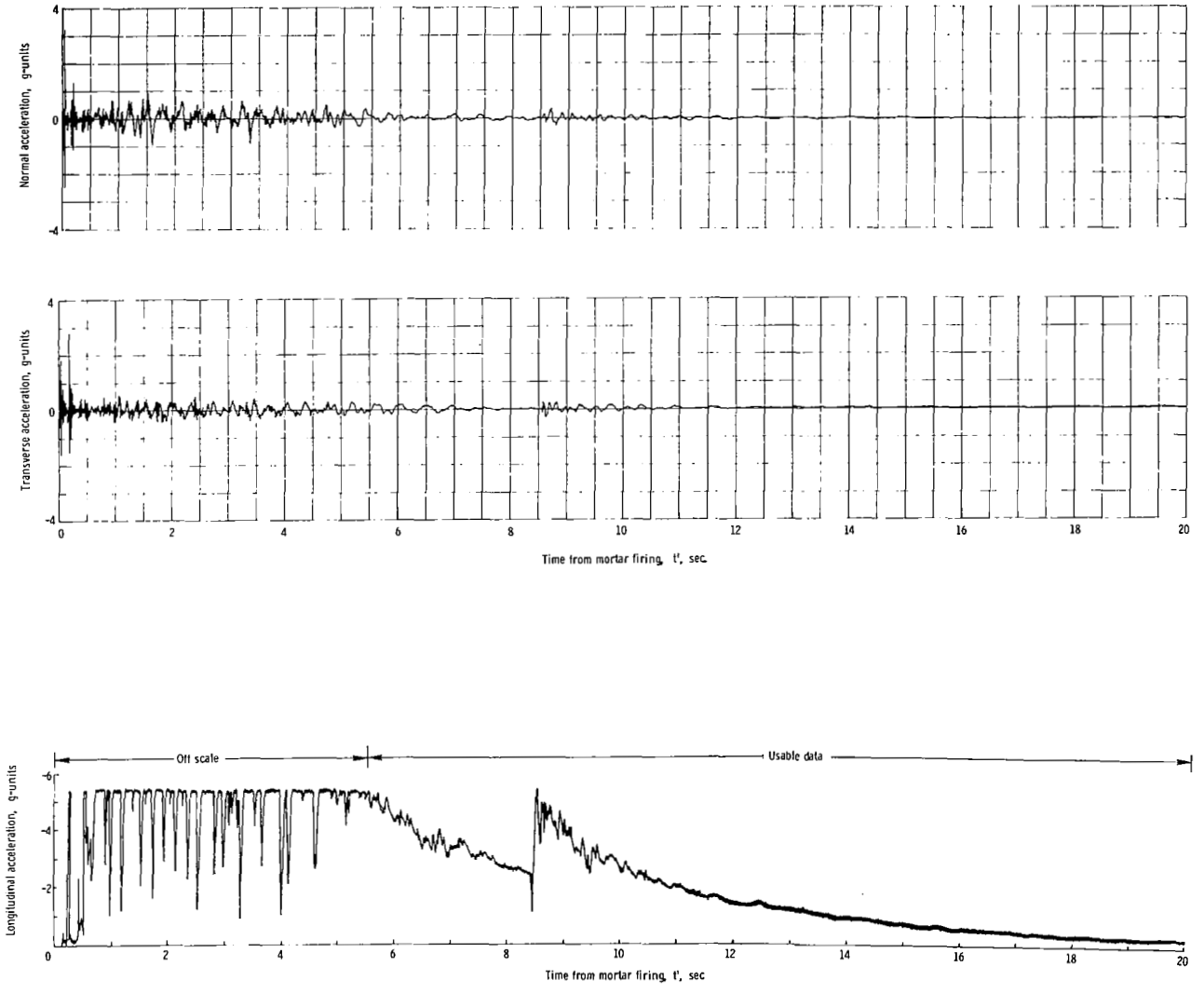

Figure 14.- Concluded.

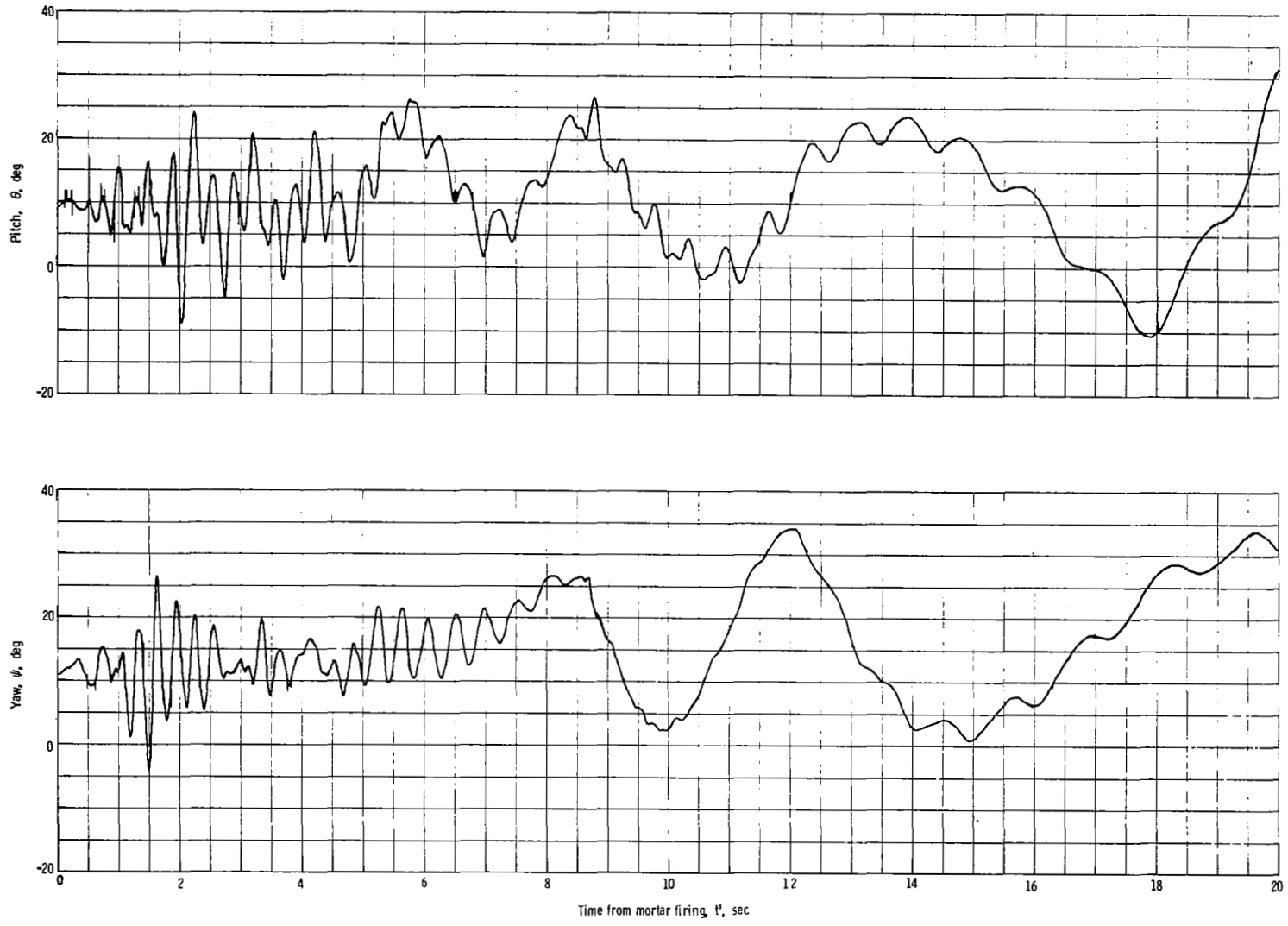

Figure 15.- Payload pitch and yaw time histories.

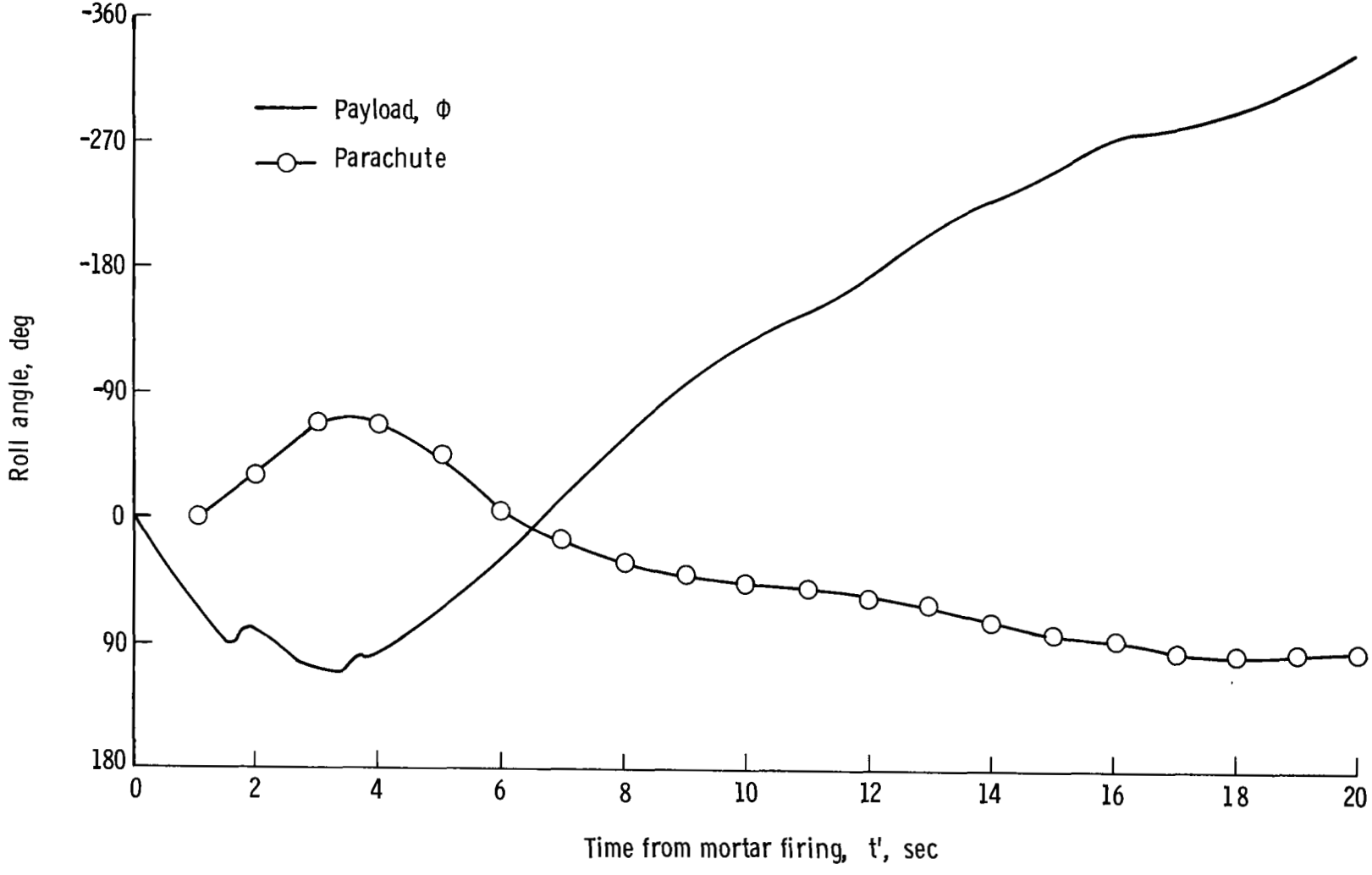

Figure 16.- Payload and parachute roll angle histories.

t' = 0.44 sec

t' = 0.57 sec

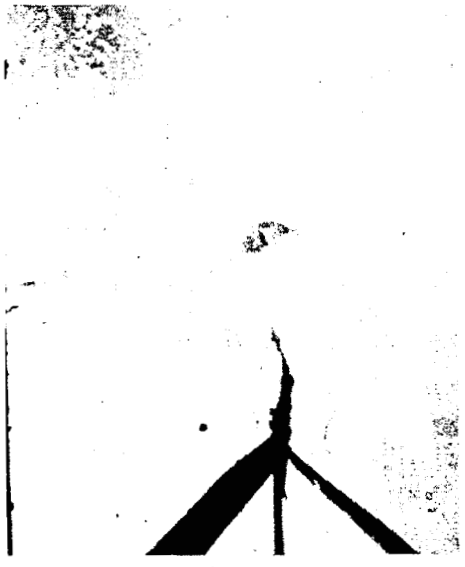

t' = 0.63 sec

t' = 0.69 sec

(a) Initial canopy inflation. L-71-669

Figure 17.- Onboard camera photographs.

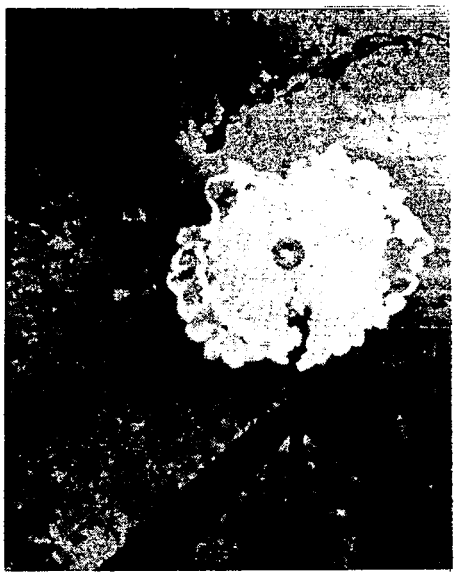

t' = 0.76 sec

t' = 0.88 sec

t' = 0.96 sec

t' = 1.04 sec

(a) Concluded. L-71-670

Figure 17.- Continued.

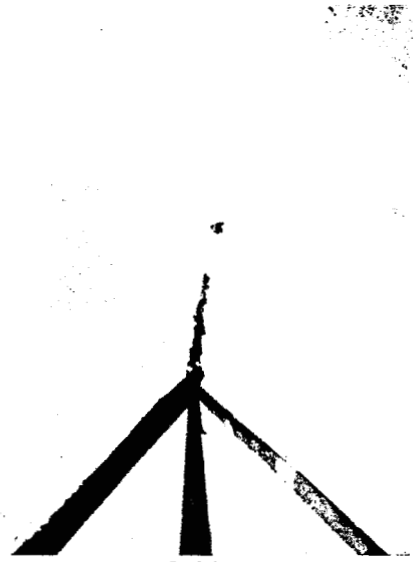

t' = 3.00 sec

t' = 3.03 sec

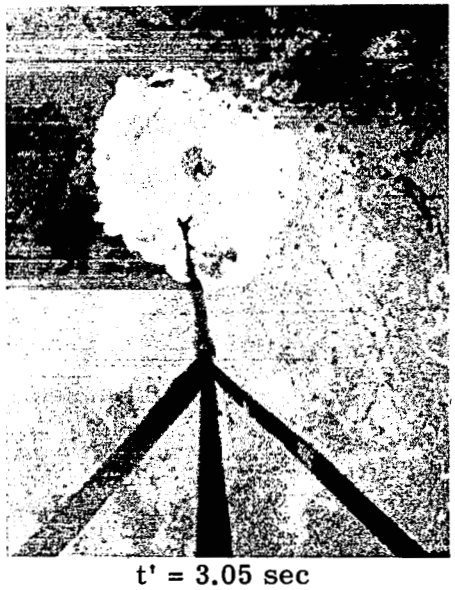

t' = 3.05 sec

t' = 3.08 sec

(b) Unsteady reefed inflation. L-71-671

Figure 17.- Continued.

t' = 6.00 sec

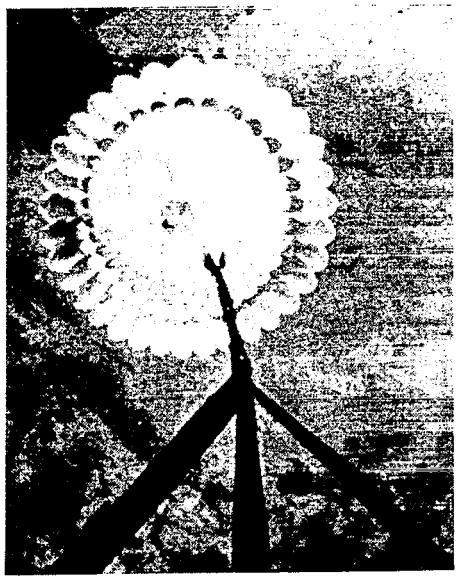

t' = 6.03 sec

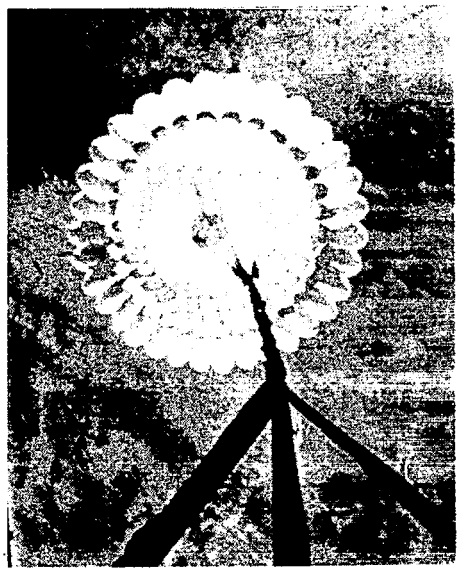

t' = 6.05 sec

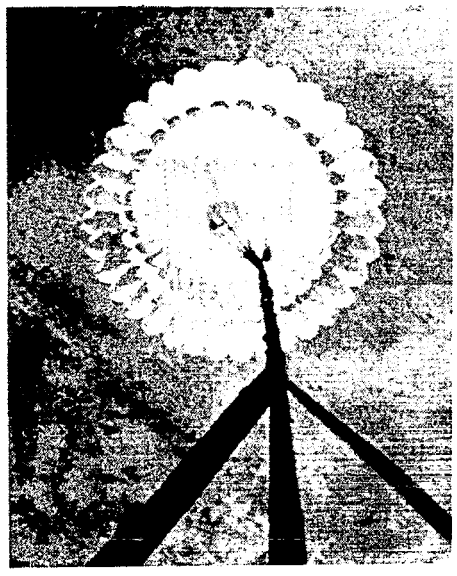

t' = 6.08 sec

(c) Steady reefed inflation. L-71-672

Figure 17.- Continued.

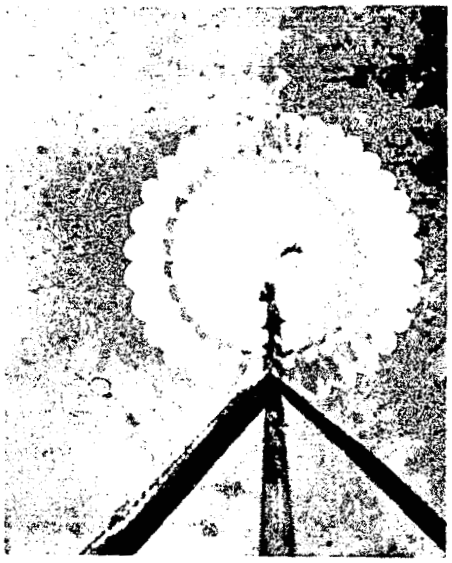

t' = 8.48 sec

t' = 8.49 sec

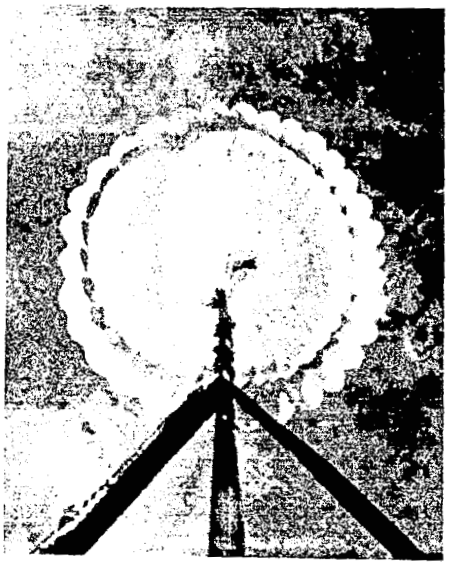

t' = 8.52 sec

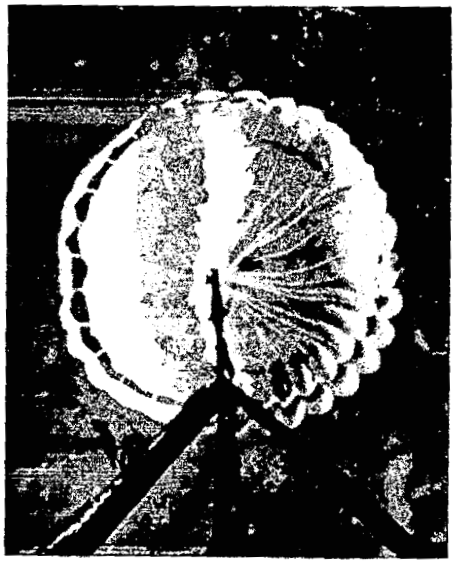

t' = 8.55 sec

(d) Disreefing sequence. L-71-673

Figure 17.- Continued.

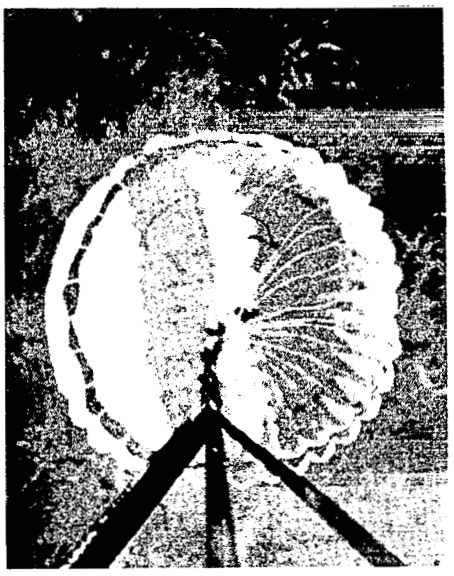

t' = 8.57 sec

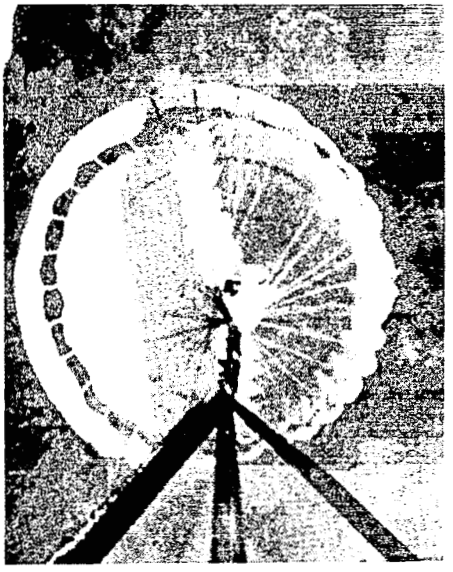

t' = 8.60 sec

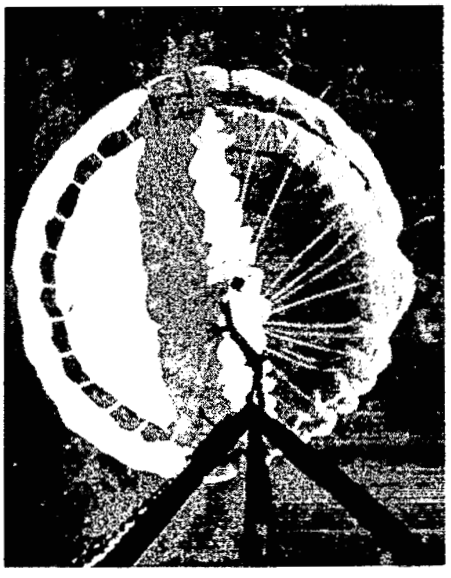

t' = 8.63 sec

t' = 8.66 sec

(d) Concluded. L-71-674

Figure 17.- Continued.

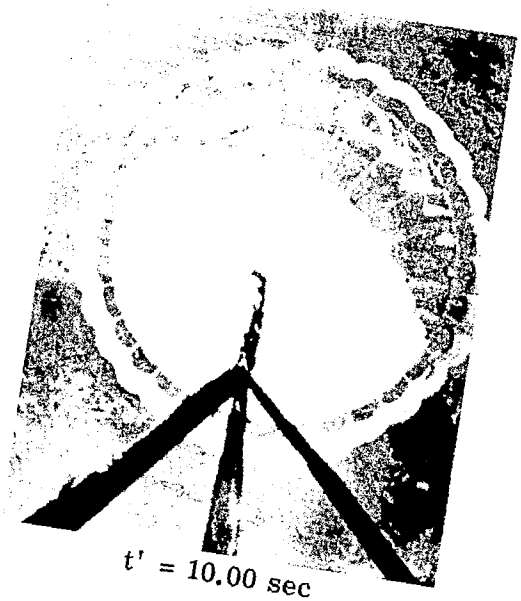

t' = 10.00 sec

t' = 10.03 sec

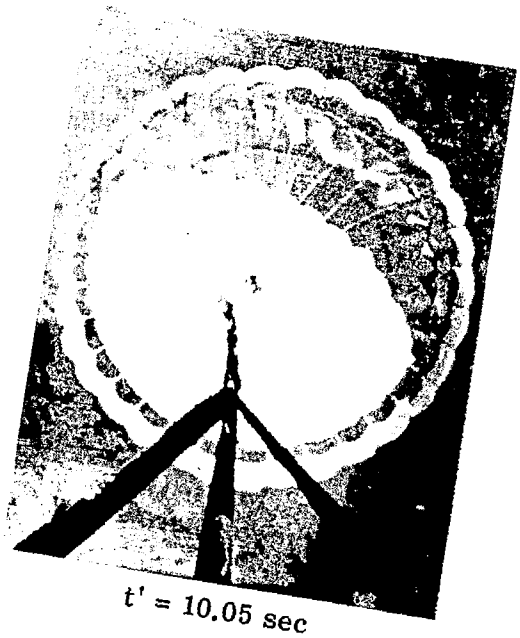

t' = 10.05 sec

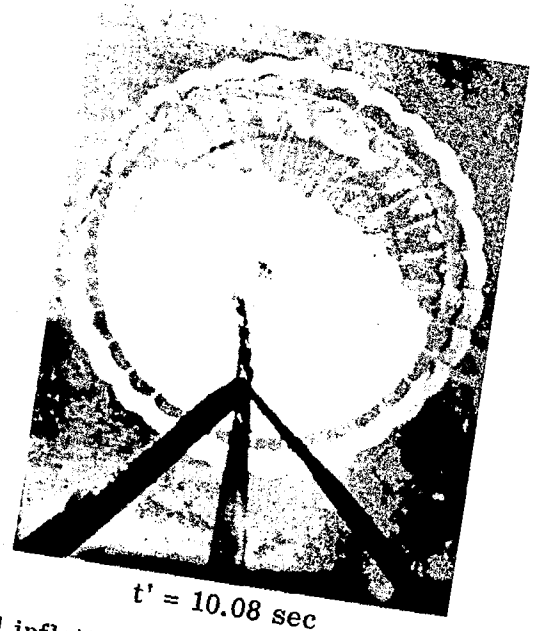

t' = 10.08 sec

(e) Steady unreefed inflation.

Figure 17.- Concluded. L-71-675

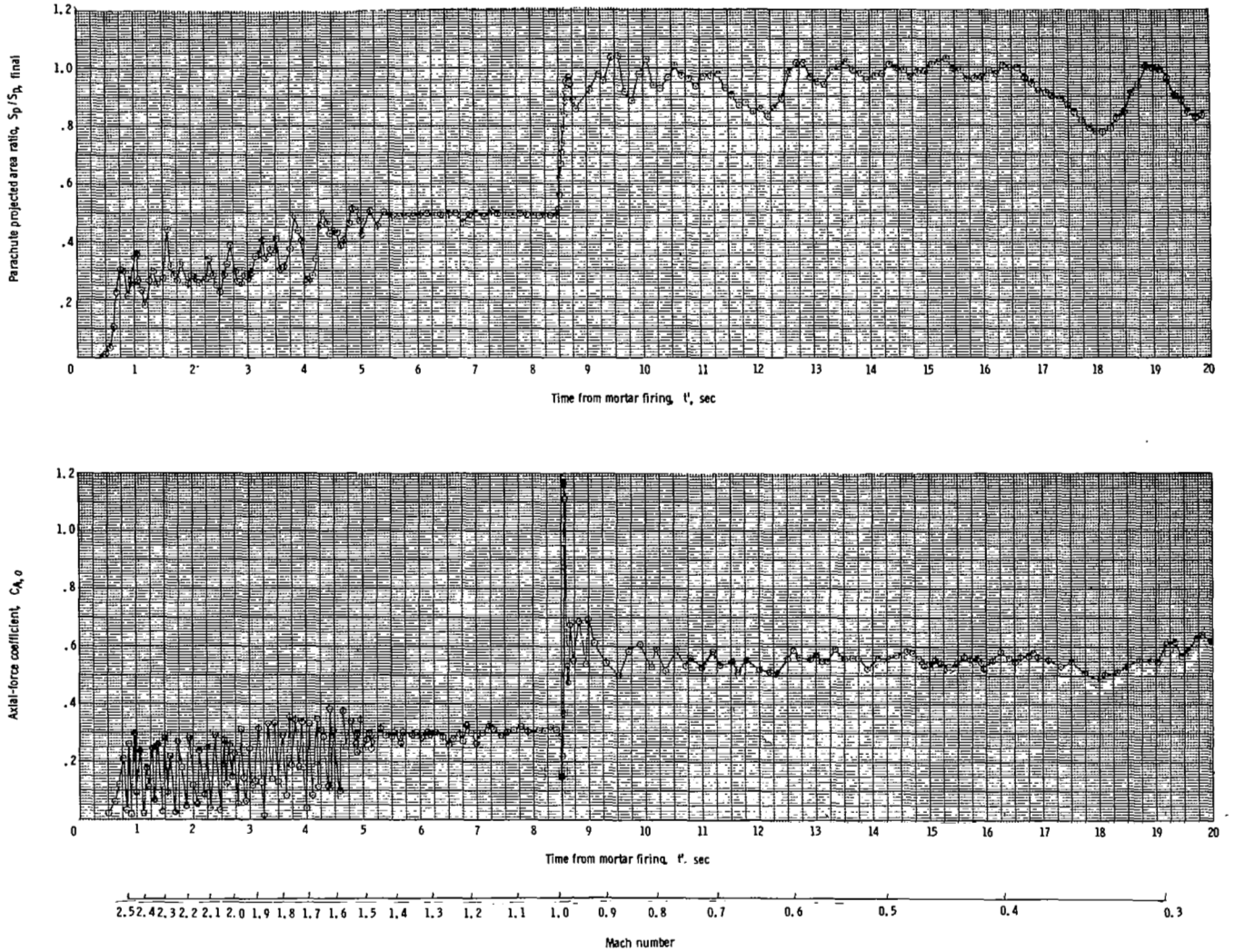

Figure 18.- Parachute projected area ratio and axial-force coefficient as a function of time and Mach number.

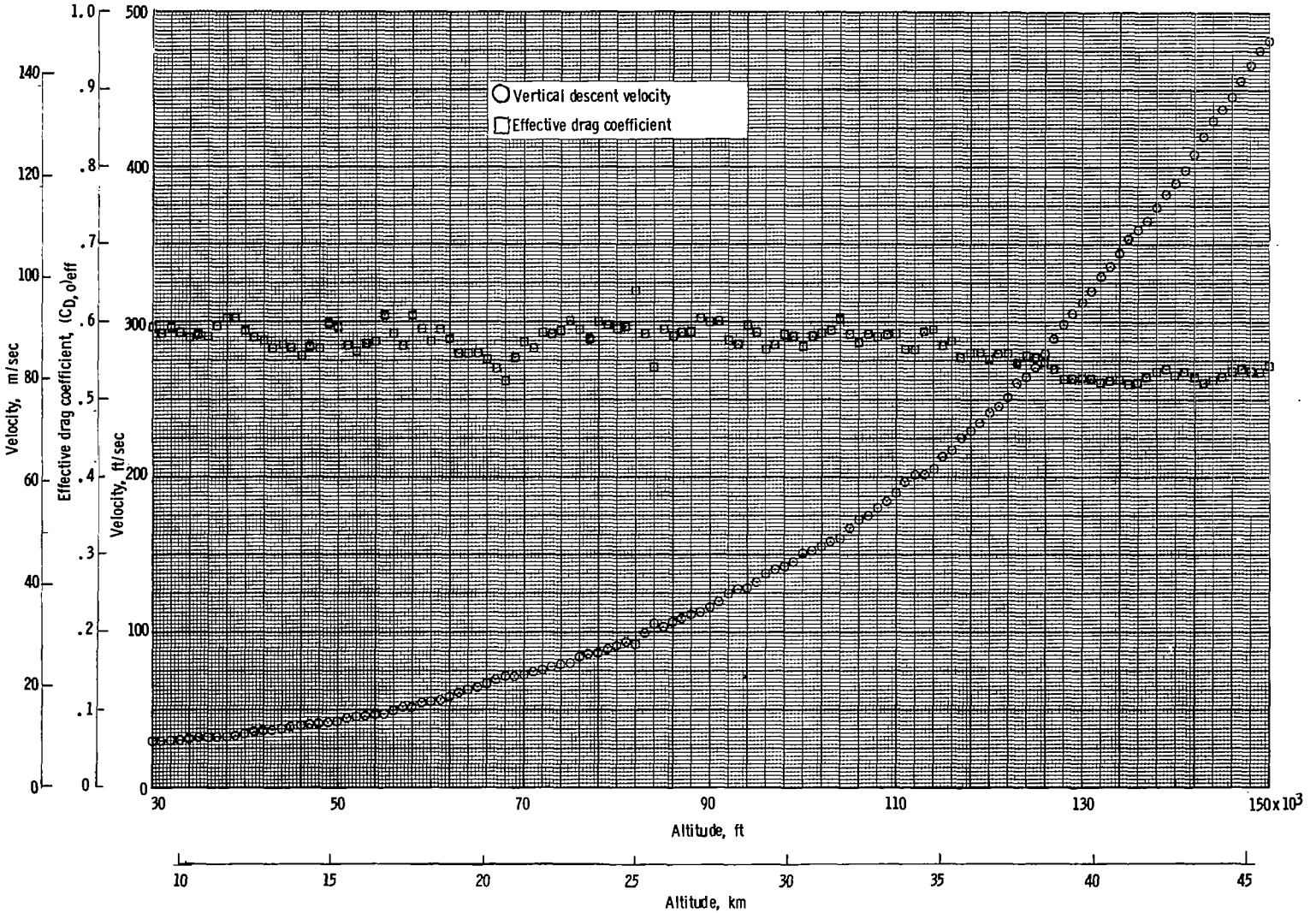

Figure 19.- Variation of vertical descent velocity and effective drag coefficient with altitude.

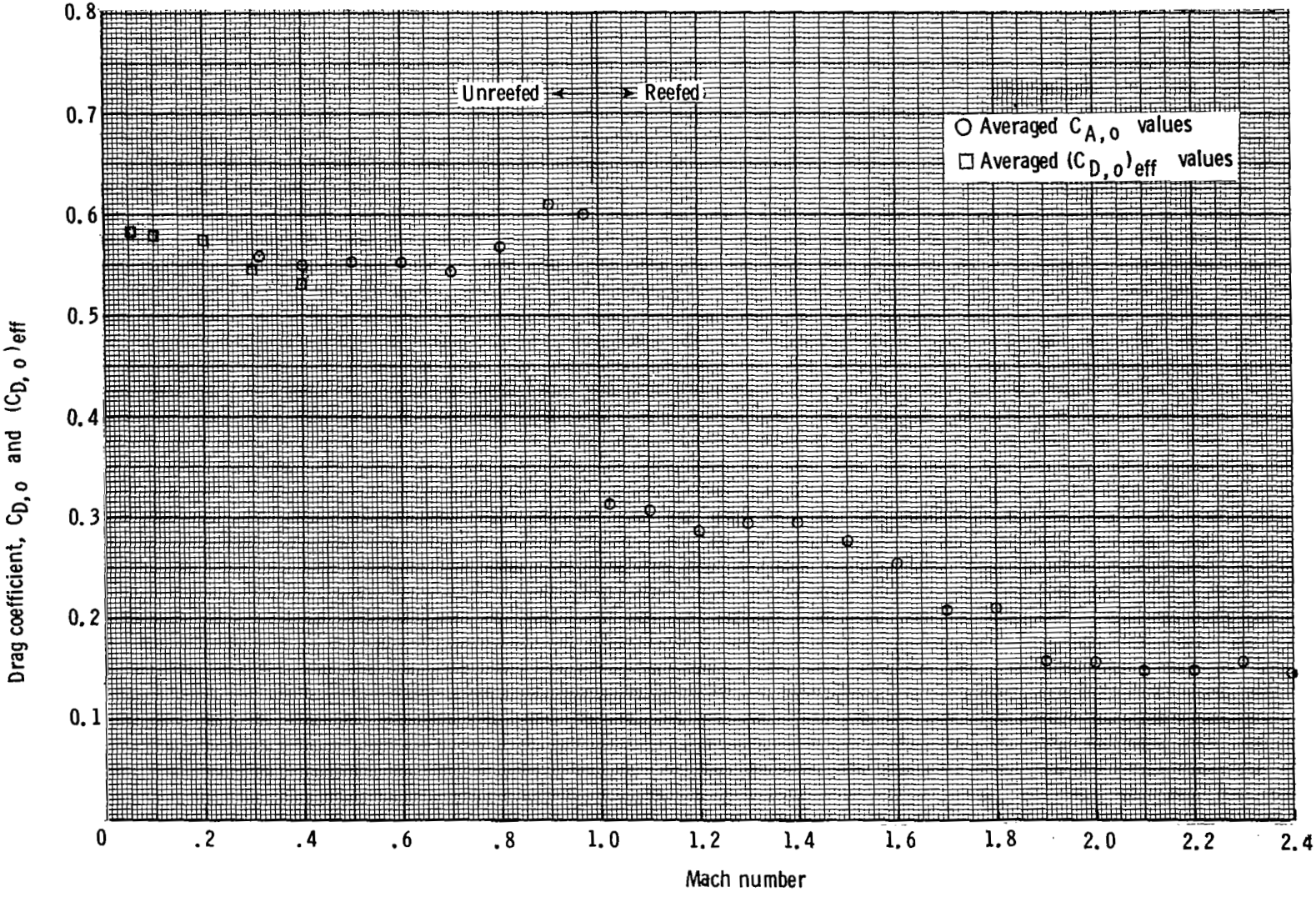

Figure 20.- Drag coefficient as a function of Mach number.

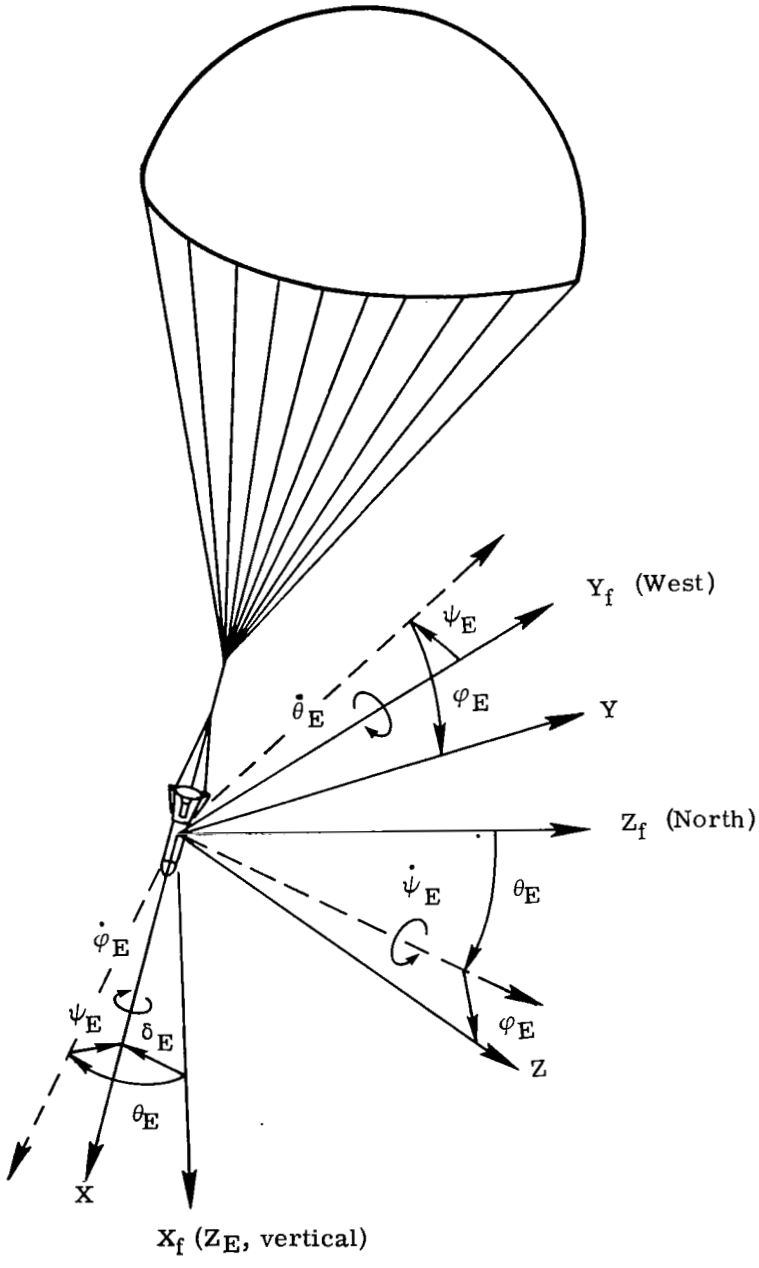

Figure 21.- Sketch showing relationship between body axes (X, Y, Z) and earth-fixed axes (X_f, Y_f, Z_f). Angles are defined in the Euler angle sense by the sequence: (1) θ_E, (2) ψ_E, (3) φ_E.

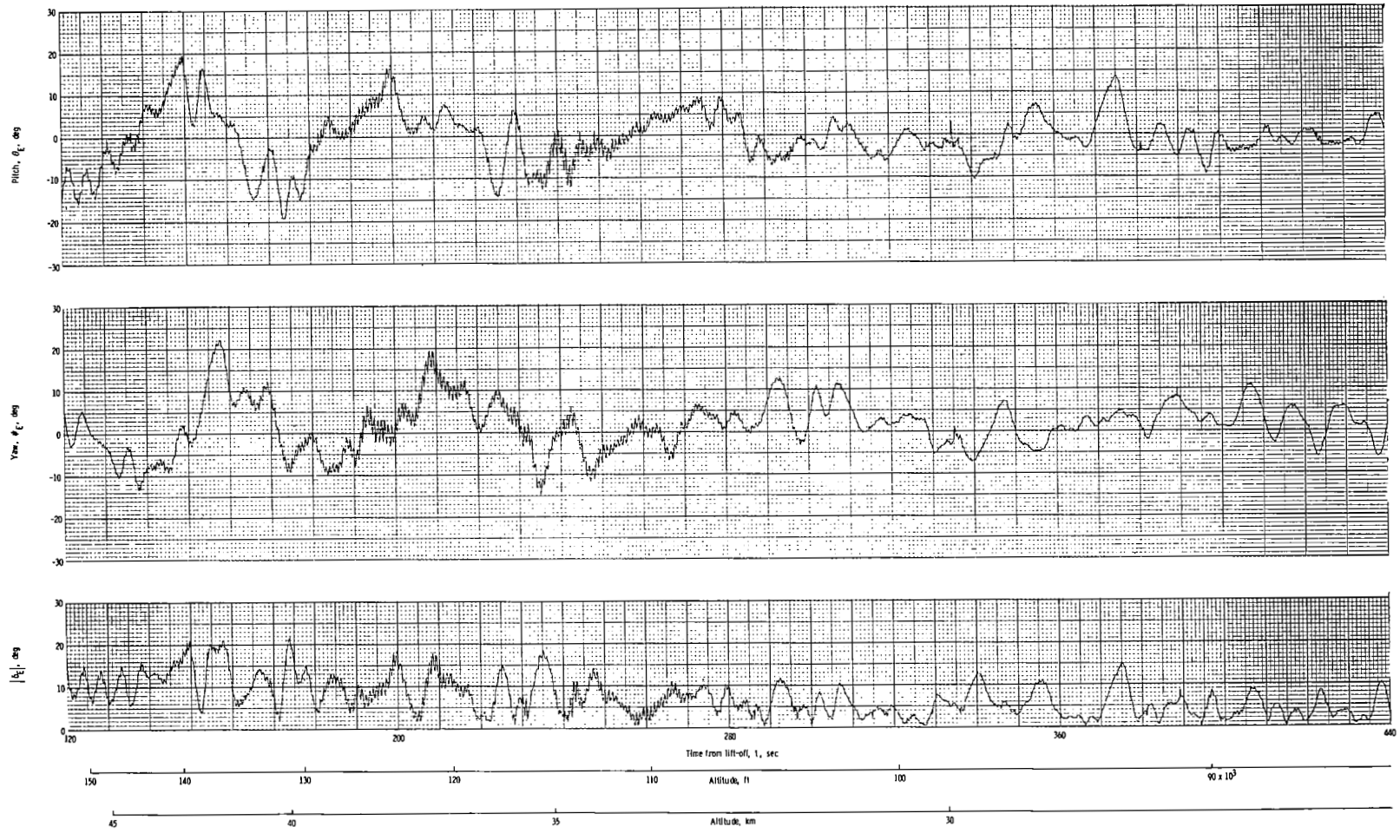

Figure 22.- Time histories of pitch θ_E, yaw ψ_E, and the resultant angle $|\delta_E|$ during descent.

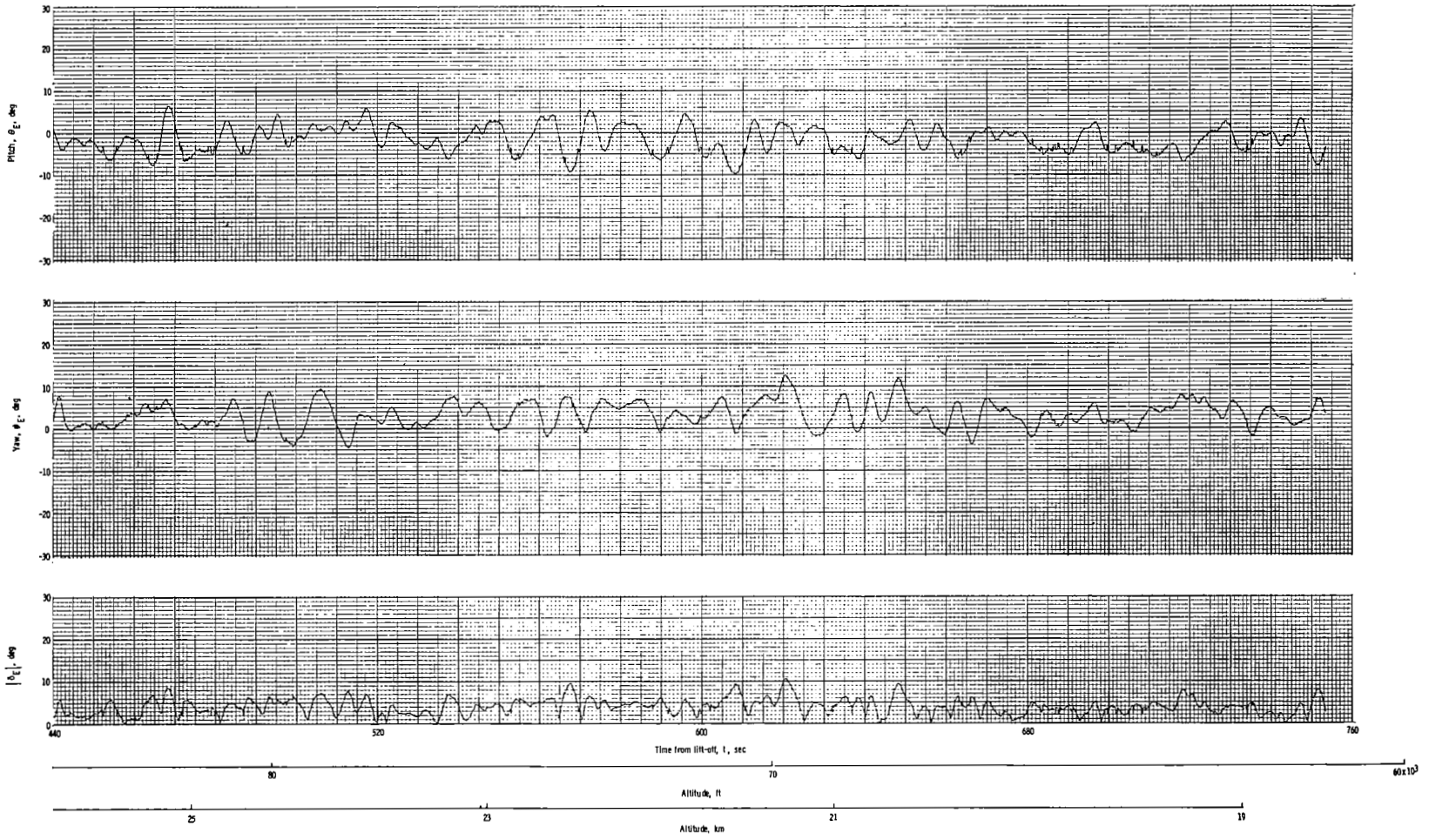

Figure 22.- Concluded.

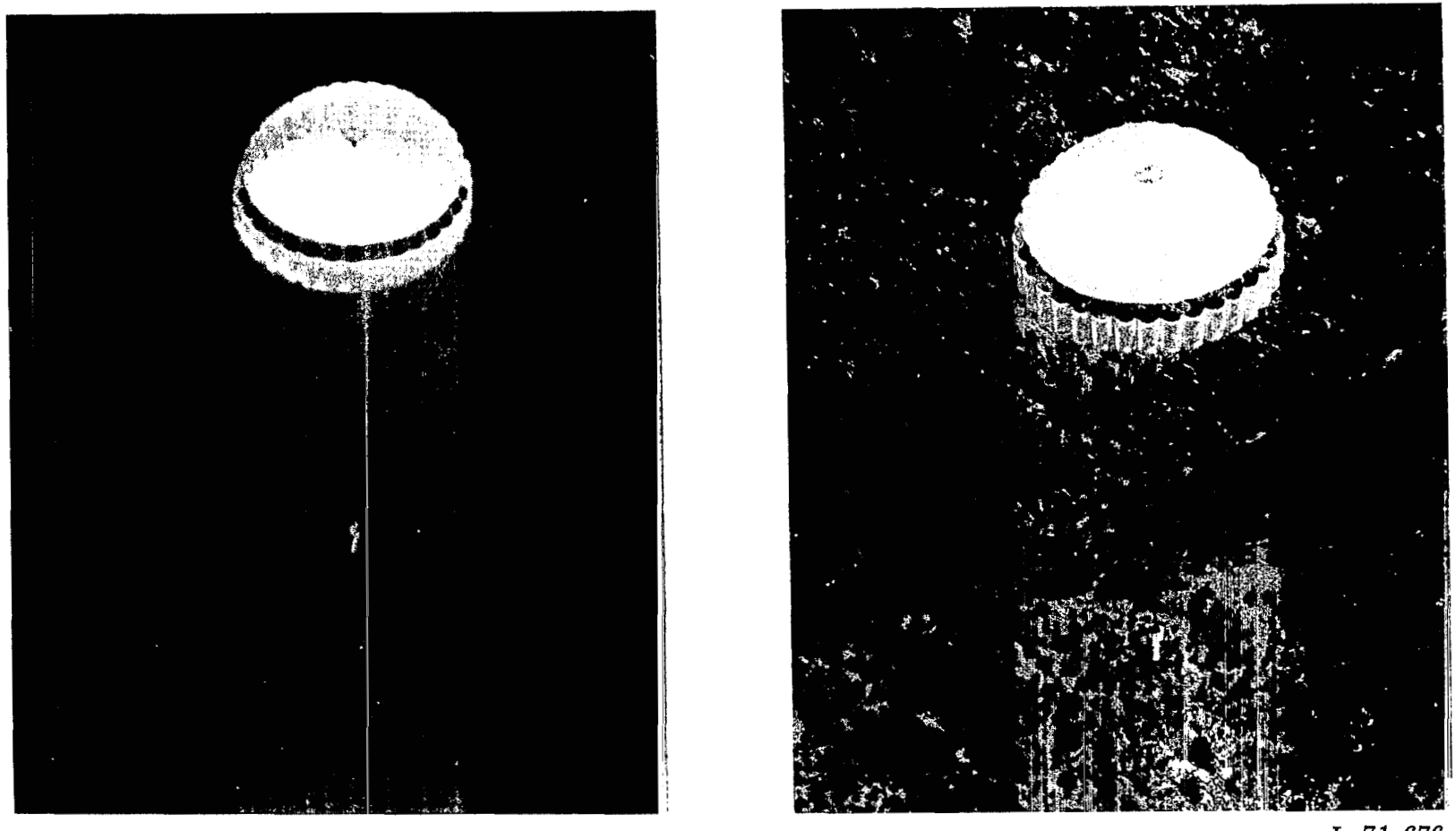

L-71-676

Figure 23.- Photographs of descending parachute near impact.

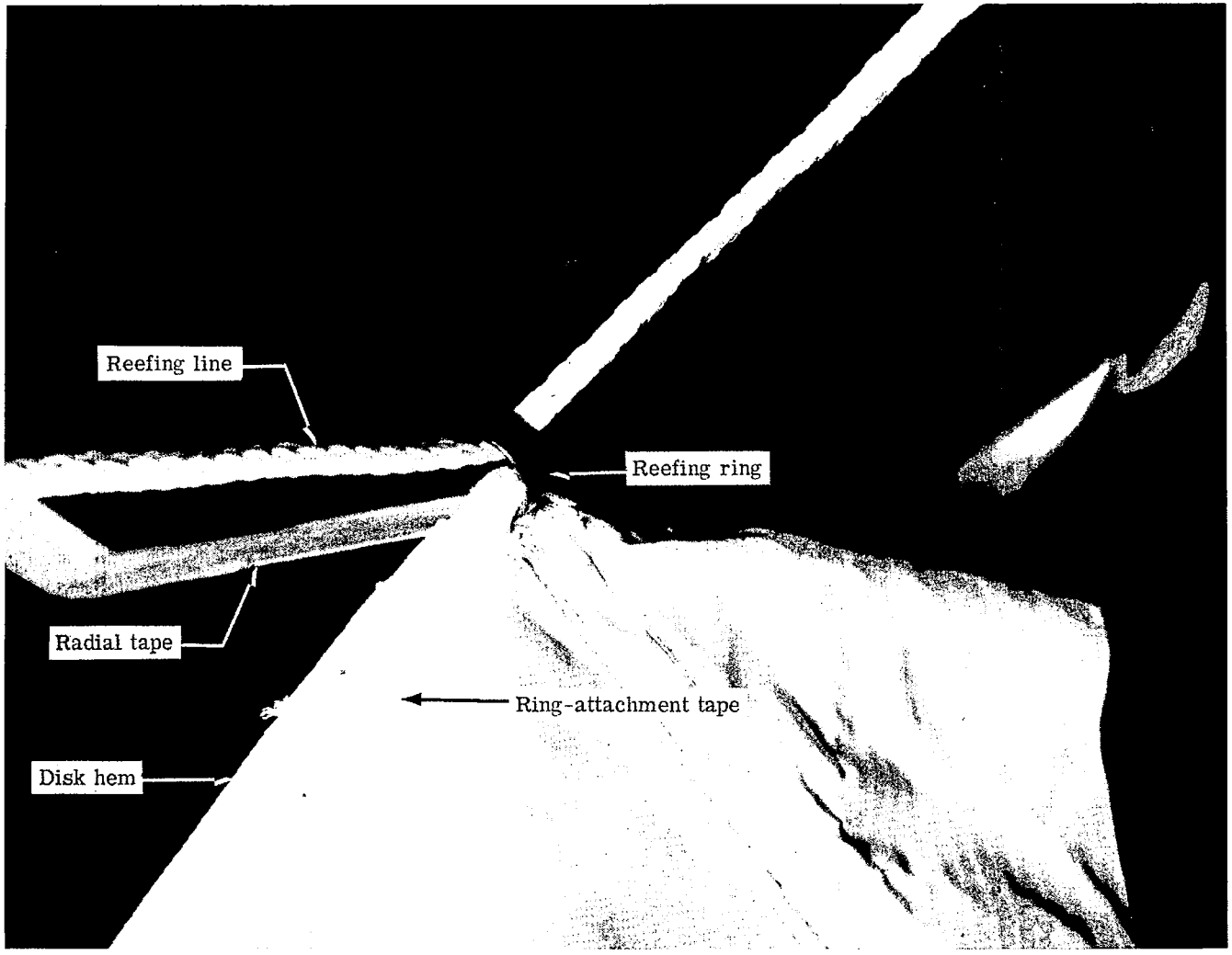

L-71-822.1

Figure 24.- Photograph of part of the reefing system.

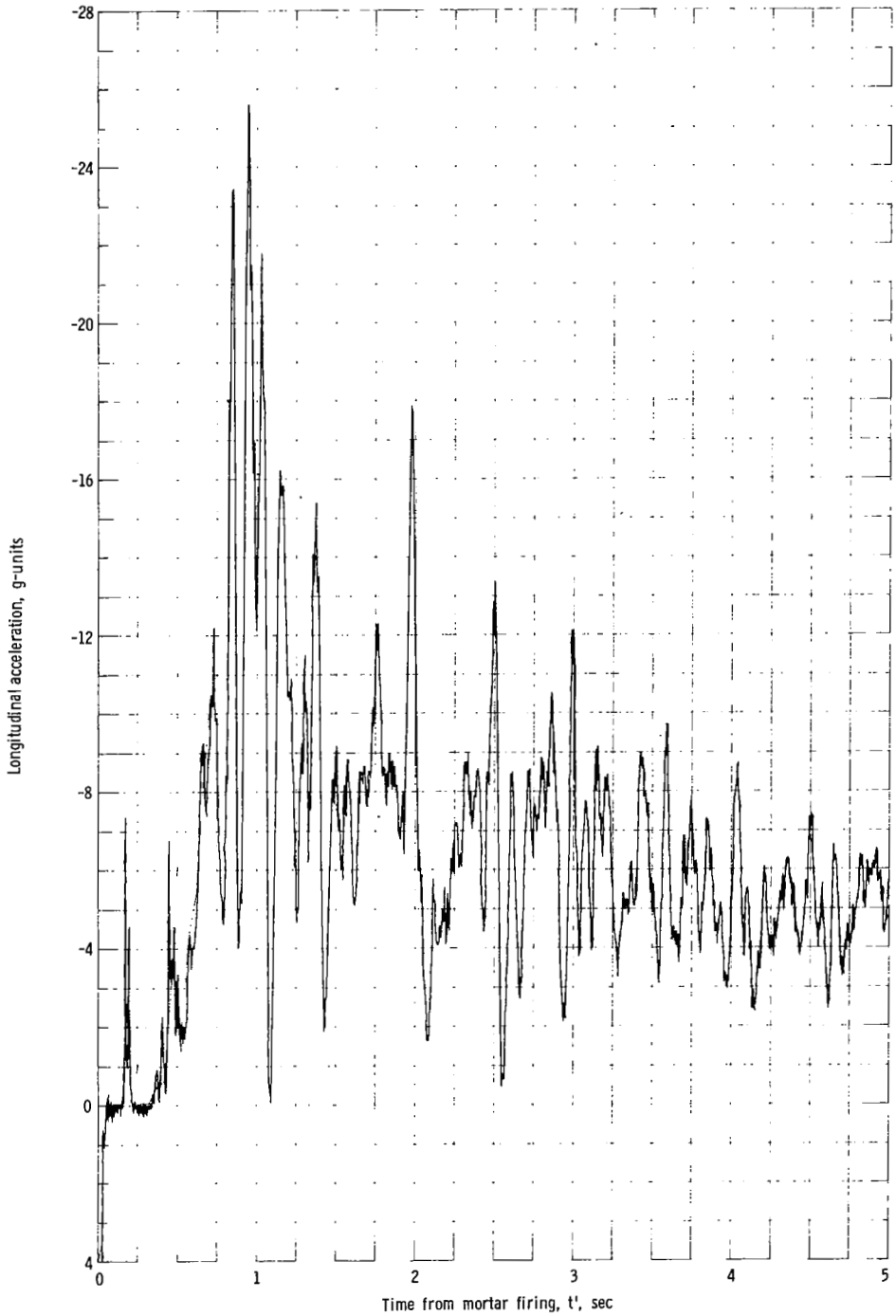

Figure 25.- Longitudinal acceleration time history.

t' = 0.45 sec

t' = 0.59 sec

t' = 0.69 sec

t' = 0.78 sec

(a) Initial canopy inflation. L-71-677

Figure 26.- Onboard camera photographs.

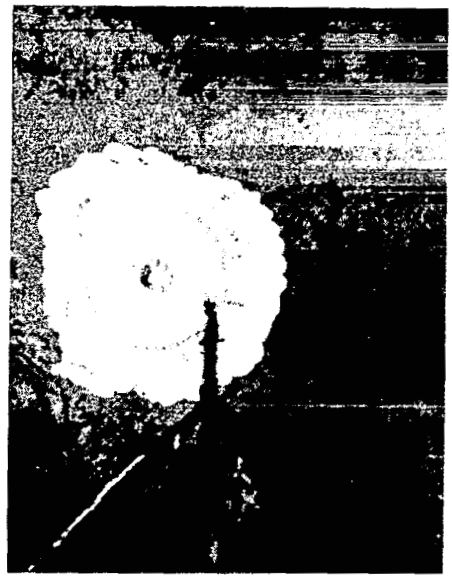

t' = 0.83 sec

t' = 0.89 sec

t' = 0.95 sec

t' = 1.06 sec

(b) Failure of reefing system. L-71-678

Figure 26.- Continued.

t' = 1.19 sec

t' = 1.28 sec

t' = 1.37 sec

t' = 1.90 sec

L-71-679

(c) Canopy damage photographs.

Figure 26.- Concluded.

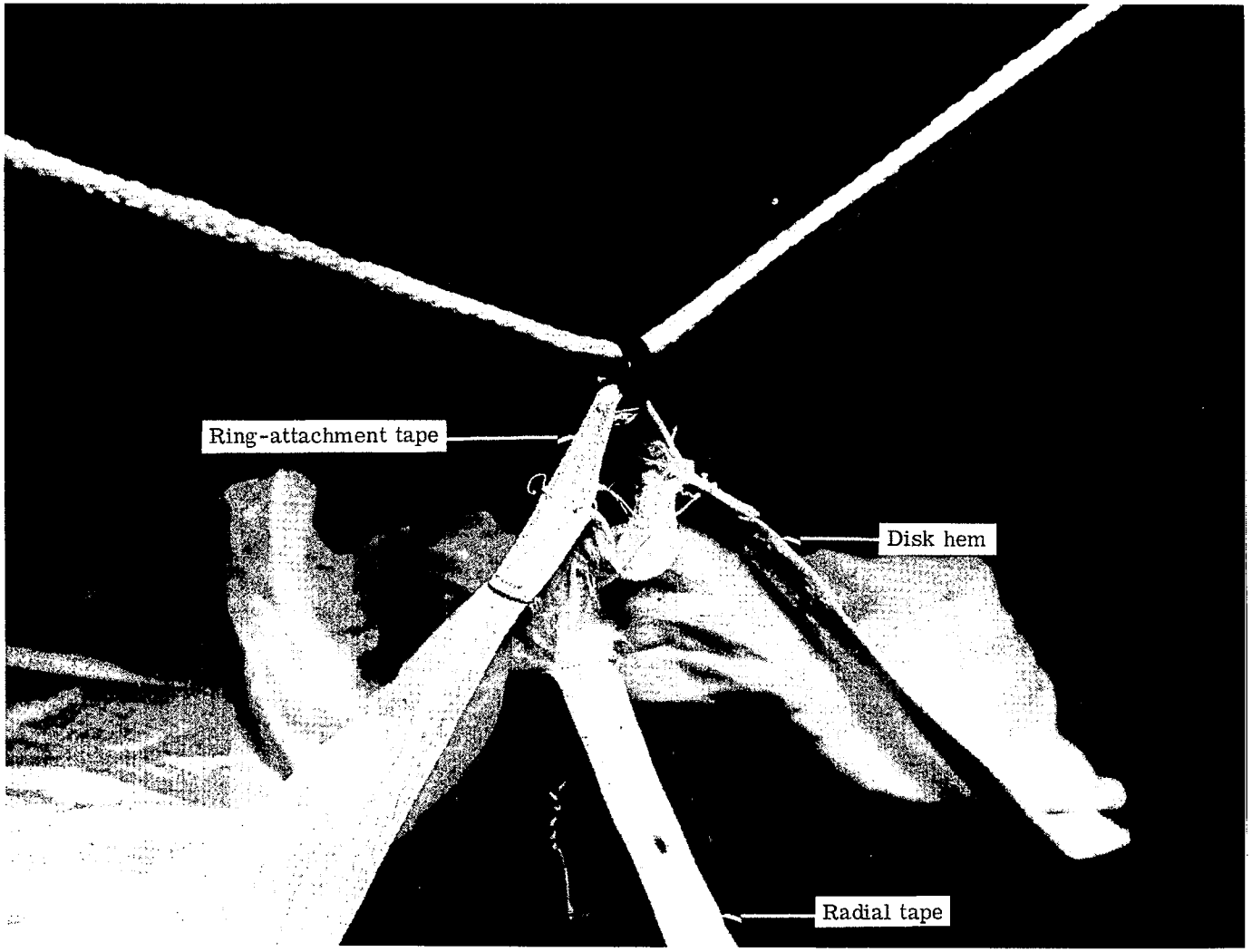

L-71-826.1

Figure 27.- Photographs of specimen undergoing tension test.

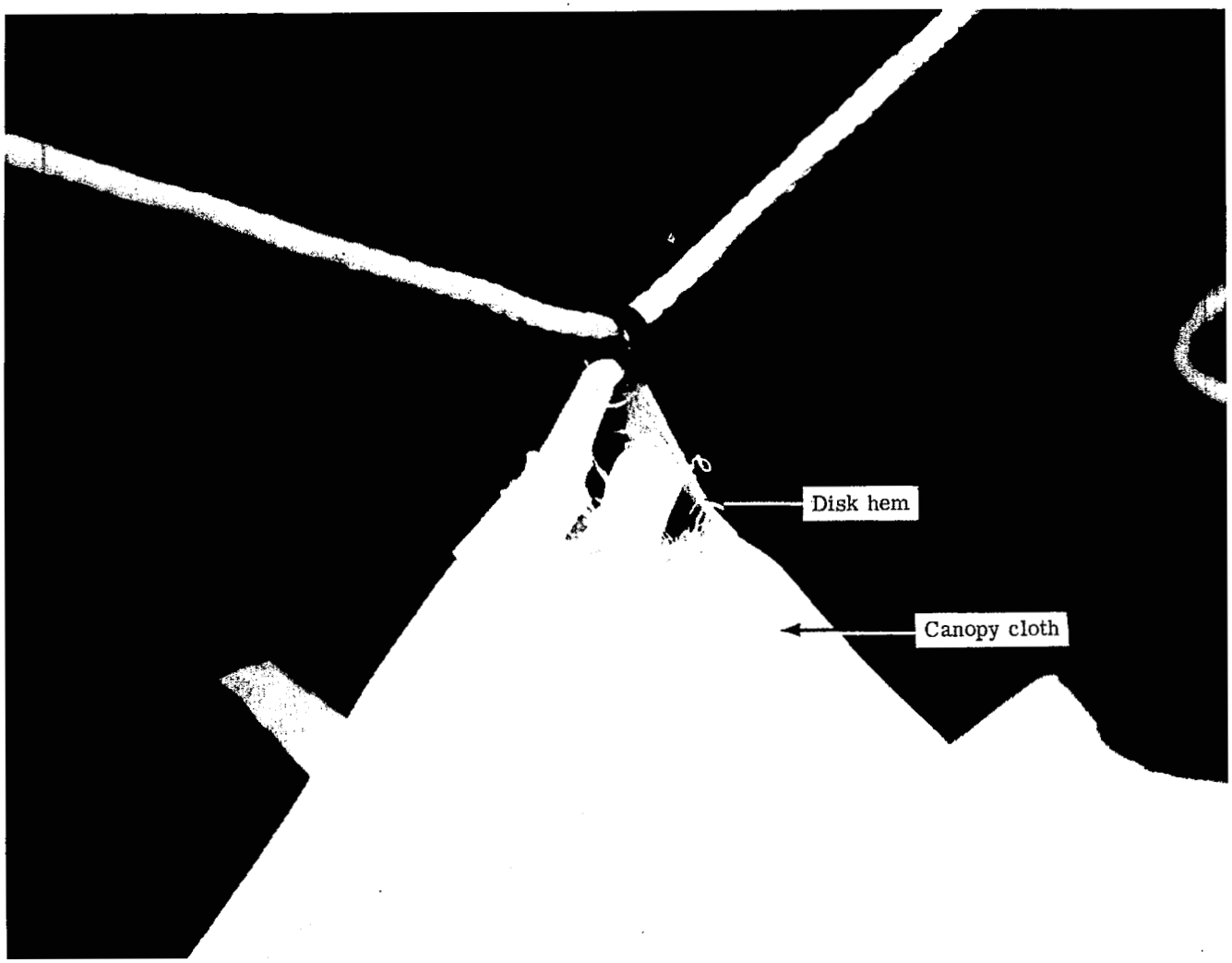

L-71-825.1

Figure 27.- Concluded.

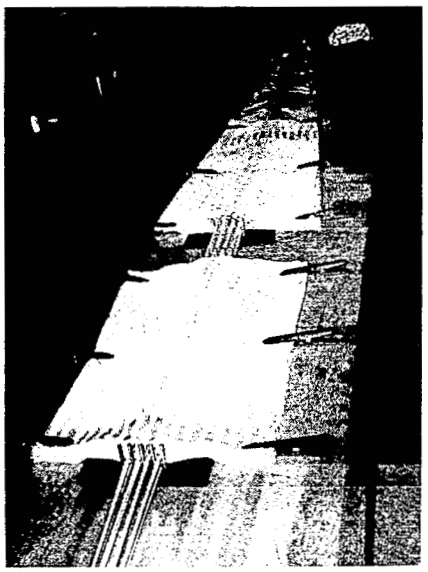

(a)

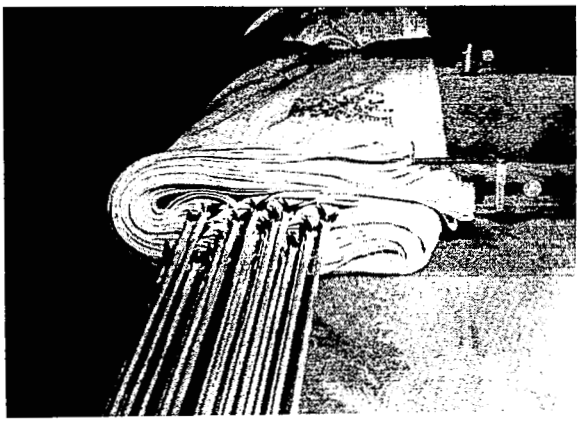

(b)

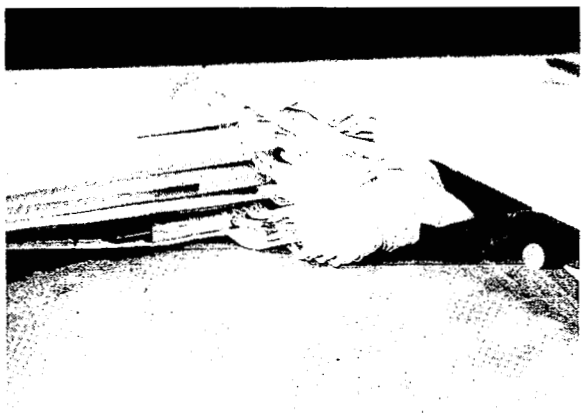

(c)

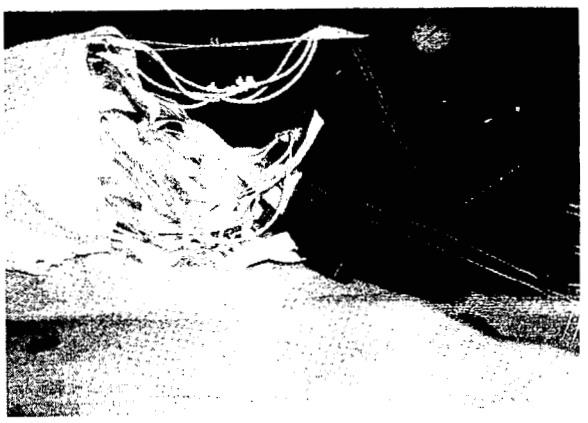

(d)

L-71-680

Figure 28.- Photographs of parachute at different stages of packing process.

(e)

(f)

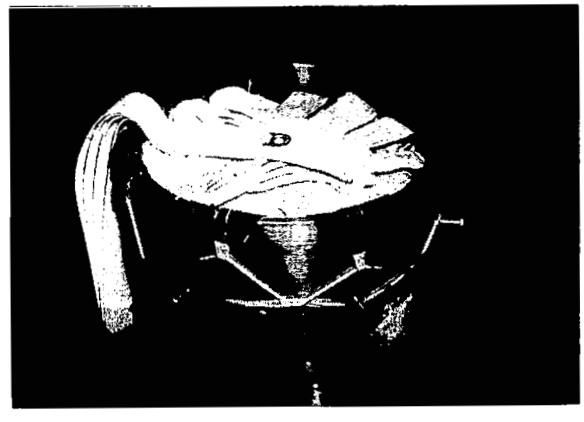

(g)

L-71-681

Figure 28.- Continued.

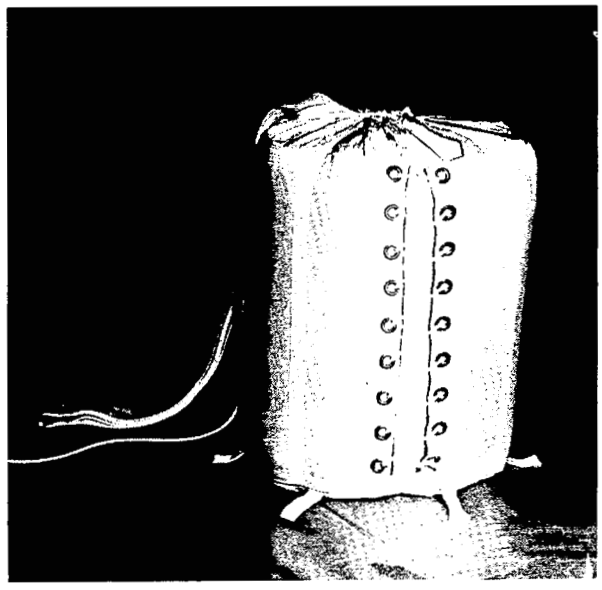

(h)

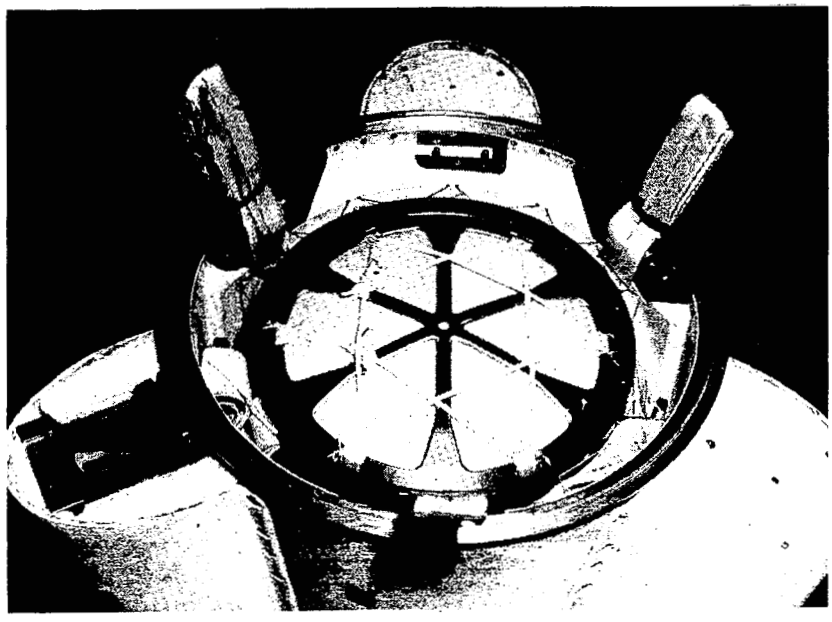

(i)

L-71-682

Figure 28.- Concluded.

NASA-Langley, 1971 — 2 L-7772

A motion-picture film supplement L-1106 is available on loan. Requests will be filled in the order received. You will be notified of the approximate date scheduled.

The film (16 mm, 5 min, color, silent) is in two sections and shows (1) the reefed 12.2-meter parachute during deployment and inflation, disreefing, and a portion of descent as taken by a camera on the aft end of the payload, and (2) a 1.7-meter disk-gap-band parachute with the same reefing geometry in a wind tunnel at $M = 2.0$ as taken by a side-viewing camera.

Requests for the film should be addressed to:

NASA Langley Research Center
Att: Photographic Branch, Mail Stop 171
Hampton, Va. 23365

CUT

Date _____

Please send, on loan, copy of film supplement L-1106 to TN D-6469.

_____
Name of organization

_____
Street number

_____
City and State Zip code

Attention: Mr. _____

Title _____

"The aeronautical and space activities of the United States shall be conducted so as to contribute . . . to the expansion of human knowledge of phenomena in the atmosphere and space. The Administration shall provide for the widest practicable and appropriate dissemination of information concerning its activities and the results thereof."

—NATIONAL AERONAUTICS AND SPACE ACT OF 1958

NASA SCIENTIFIC AND TECHNICAL PUBLICATIONS

TECHNICAL REPORTS: Scientific and technical information considered important, complete, and a lasting contribution to existing knowledge.

TECHNICAL NOTES: Information less broad in scope but nevertheless of importance as a contribution to existing knowledge.

TECHNICAL MEMORANDUMS: Information receiving limited distribution because of preliminary data, security classification, or other reasons.

CONTRACTOR REPORTS: Scientific and technical information generated under a NASA contract or grant and considered an important contribution to existing knowledge.

TECHNICAL TRANSLATIONS: Information published in a foreign language considered to merit NASA distribution in English.

SPECIAL PUBLICATIONS: Information derived from or of value to NASA activities. Publications include conference proceedings, monographs, data compilations, handbooks, sourcebooks, and special bibliographies.

TECHNOLOGY UTILIZATION PUBLICATIONS: Information on technology used by NASA that may be of particular interest in commercial and other non-aerospace applications. Publications include Tech Briefs, Technology Utilization Reports and Technology Surveys.

Details on the availability of these publications may be obtained from:

SCIENTIFIC AND TECHNICAL INFORMATION OFFICE

NATIONAL AERONAUTICS AND SPACE ADMINISTRATION

Washington, D.C. 20546